# Development of Advanced Deposition Technology for Nanocrystalline Si Based Solar Cells and Modules

# Annual Technical Progress Report

covering period

May 1, 2002 – June 30, 2003

Subcontract No. ZDJ-2-30630-28

Under

Prime Contract No. DE-AC36-99-GO10337

Under the *Thin Film Photovoltaics Partnership Program*


Prepared by:

Yuan-Min Li

With contributions from

J.A. Anna Selvan and A.E. Delahoy

Energy Photovoltaics, Inc.
P.O. Box 7456, Princeton, NJ 08543

In collaboration with lower-tier subcontractor

A. Rafik Middya and E.A. Schiff

Department of Physics, Syracuse University
Syracuse, NY 13244


Submitted to:

Dr. Bolko von Roedern, Contract Technical Monitor

National Renewable Energy Laboratory
1617 Cole Boulevard
Golden, CO 80401-3393

July 25, 2003

# Executive Summary

Our primary objective in Phase I of the three-year subcontract with NREL was to demonstrate the viability of nanocrystalline silicon (nc-Si) p-i-n type solar cell processing in a low cost, single-reactor system by conventional RF-PECVD on commercial grade $SnO_2$ substrates. Good FF and $V_{oc}$ were used as yardsticks for the performance of solar cells containing nc-Si i-layers, while the important device optical engineering ($J_{sc}$) was relegated to future efforts.

We report on the key activities centered on the search for a robust process for high performance nc-Si single junction solar cells deposited entirely in a one-chamber, batch-process type RF-PECVD system using the hydrogen dilution method. Conversion efficiency of 5% has been obtained on commercial grade $SnO_2$-coated, 3-mm thick soda-lime glass superstrates, using simple Al back contact. The most critical element in device processing has been found to be the seeding procedure by which nc-Si:H absorber (the i-layer) is grown over an amorphous-Si based underlayer. Seeding by boron-doped p-layer leads to superior devices of excellent stability than seeding inside i-layer. Both types of seeding methods remain to be optimized. We have vigorously tackled the problem of phosphorus cross-contamination of the nc-Si absorbers, and improved device reproducibility. Ar dilution (without hydrogen) is capable of producing nc-Si films ill suited for solar cells. We have started to work on tunnel junction processes that satisfy low-contamination requirement for a-Si/nc-Si tandem devices. An extremely critical question for device performance and uniformity is why superior nc-Si solar cells are made *only* with nc-Si absorbers grown near the boundary (the 'edge') of transition to the amorphous phase.

In parallel to the device research at EPV, our lower-tier subcontractor at Syracuse University has completed the setup for combined plasma and hot-wire CVD. Preliminary Si:H film depositions have been made in the PECVD mode. Infrared photocurrent spectroscopy has been developed and applied to estimating defect density of absorber layers of nc-S:H single junction solar cells.

The moderate success of our initial efforts has partially validated our approach and given us a good deal of confidence in furthering our efforts in such critical and challenging areas as seeding layer optimization, device reproducibility and contamination control, tunnel junction with low cross contamination, device uniformity (scaling up), higher growth rates, and more advanced optical engineering for higher $J_{sc}$. Most, if not all, of these elements must be in place in order for us to reach the lofty, final goal of this subcontract: high efficiency a-Si/nc-Si tandem PV modules by an unconventional, relatively low cost process (the 'cheap and dirty' way).

# Table of Contents

## List of Figures



## List of Tables

## 1.0 Introduction

Solar cells based on nanocrystalline silicon (nc-Si:H, commonly known as micro-crystalline silicon or μc-Si:H) absorbers have shown promising efficiencies in single junction and double junction photovoltaic devices including large area modules [1-4], with good long-wavelength absorption and superior stability against light soaking. As a replacement for a-SiGe:H alloy, nc-Si is well suited as the bottom absorber in stacked a-Si/nc-Si tandem solar cells. The narrow-gap nc-Si absorber can capture more red-light than a-SiGe:H for higher $J_{sc}$, and does not require expensive $GeH_4$ feedstock. Additionally, due to the thicker i-layer of the nc-Si bottom cell, reduction in shunting can be expected to significantly benefit the manufacturing of large-area PV modules. The a-Si/nc-Si type device is one of the most promising thin film candidates for cost-competitive photovoltaic applications in terms of efficiency improvement, scale-up potential, raw material availability, energy payback time, and performance under outdoor conditions.

High efficiency p-i-n type single junction nc-Si:H solar cells are normally grown on expensive, laboratory superstrates, such as the Asahi type 'U' $SnO_2$ or custom ZnO-coated glass of high texture and low absorption. Also standard is the use of a highly effective back reflector such as ZnO/Ag, or efficient diffuse back reflectors such as surface textured ZnO [5]. The high-efficiency 'champion' devices made by the PECVD methods [2-4] were invariably prepared in sophisticated (read: expensive), multi-chamber, and/or load-locked deposition systems. The electrode utilization efficiency, which is defined as the surface area ratio of the powered electrode to that of the substrates, is typically low at about one (1:1). To evaluate the true potential of nc-Si:H absorbers for cost-competitive, *commercially viable* manufacturing of large-area photovoltaic (PV) modules, we have taken a realistic approach, based on our proven industrial production of 8 $Ft^2$ a-Si:H PV modules by a massively-parallel batch process in single chamber RF-PECVD systems [6], to the study of nc-Si:H solar cells, with the ultimate aim of manufacturing tandem a-Si/nc-Si devices. We have attempted to address several practical issues facing nc-Si:H PV technology: 1) Costly UHV type multi-chamber reactors (typically with load-lock) that is widely assumed to be necessary to prevent impurity and/or dopant contamination; 2) Low deposition rate per unit area of powered-electrode; 3) Use of expensive, special substrates.

Under the present NREL subcontract, we have been undertaking a highly ambitious task to fabricate nc-Si devices in a *single* reactor, non-load-locked, multiple parallel-substrate PECVD system (without the gas-dispersing showerhead facing the substrate that is found in conventional PECVD reactors) on low-cost $SnO_2$-coated glass superstrates. Our R&D system dedicated to this project is a 'miniature' version of the batch-type PECVD system being deployed for the manufacturing of 0.79 $m^2$ a-Si/a-Si tandem PV modules at a rate of 48 plates per deposition run (massively-parallel processing with 12 simultaneously powered electrodes in the same substrate carrier). It was very critical for us, in the early stages of the subcontract, to gain credibility by demonstrating the 'proof-of-concept' for our uniquely challenging approach.

During Phase I, our overall goal was to lay a solid foundation for advanced research in nc-Si based solar cells by broadly exploring device fabrication recipes and identifying process issues critical to device performance. Specifically, our primary objectives are to 1) Provide evidence for single reactor/single chamber RF-PECVD nc-Si device fabrication capability by producing single junction nc-Si solar cells with good fill factor (FF) and reasonable efficiency without advanced optical engineering; 2) Identify key process requirements for device reproducibility, efficiency improvements and scaling-up to modules; 3) Obtain some empirical understanding

about nc-Si device performance and absorber properties; 4) Build the apparatus for growing nc-Si by the combined PECVD and HWCVD method at Syracuse University (SU). We have succeeded in making highly stable nc-Si:H p-i-n single junction solar cells of ~5% efficiency, in a single chamber reactor, on low-cost $SnO_2$ substrates, using simple Al back contact (without the aid of a good rear reflector such as ZnO/Al). Seeding method, gas impurity and contamination control, and degree of crystallinity are among the critical issues affecting solar cell performance. Both p-seeding and i-seeding methods have been developed, the former having the performance advantage for now. Presently, the biggest problem with of our nc-Si PV devices is the low $J_{sc}$ attributable to optical loss in the p-seeding layer, and to the deficiency in light trapping (enhancement of optical absorption in i-layer). We have started to develop tunnel junction recipes for a-Si/nc-Si tandem solar cells. The combined plasma and hot-wire CVD apparatus at SU has been completed. Very informative correlations between device performance and the microstructural and optical properties of the nc-Si absorbers have been made.

# 2.0 Descriptions of Experimental Approaches and Equipment Development

## 2.1 General approach and device structure at EPV

The work at Energy Photovoltaics, Inc. (EPV) has focused on nc-Si *device* preparation using conventional RF-PECVD in a single-chamber system. The work at our lower-tier subcontractor, Syracuse University (under the directions of Professors A.R. Middya and E.A. Schiff) has been devoted to the novel growth technique of combining PECVD with hot-wire CVD (HWCVD), simultaneously in the same reactor. Devices have been characterized at both EPV and SU. In addition, through collaborations between EPV and the New Jersey Institute of Technology (NJIT, Mr. Liwei Li and Professor R.A. Levy), the microstructures of a number of nc-Si single junction solar cells have been evaluated and correlated with their solar cell parameters.

EPV's R&D RF-PECVD system, the workhorse for the present subcontract, was constructed to closely resemble EPV's much larger manufacturing PECVD system currently used for producing large area (25"x49") a-Si:H/a-Si:H tandem (and single junction) PV modules using massively parallel, batch processing technology, by simultaneously energizing 12 RF electrodes installed in the same reactor-box (or substrate-carrier) that holds 48 substrates (four substrates for each powered electrode of about the same size). The R&D reactor, having the same design as the larger production machine, contains only a single RF-power electrode, and its dimensions are proportionally scaled down to hold four substrates of 12"x15" each in size. The reactor is placed in a single-chamber vacuum system without any load-lock chamber. External channel strip heaters are placed on the outer side-walls of the chamber for radiative heating of the interiors of the chamber. RF power at the conventional 13.56 MHz, capacitively coupled (the parallel-plate configuration) to the plasma between two pairs of substrates (one pair placed on each side of the power electrode), is supplied by an ENI ACG-6B power generator and conditioned by an RF impedance matching network (the matchbox). The single chamber design dictates that the chamber vacuum is broken after *each* deposition run for substrate removal and replacement. Very high vacuum levels have been impossible to obtain due to routine atmospheric exposure, especially in the hot and humid summer days. During earlier experiments, severe instability of the ENI automatic RF matching network (model MW-10D) caused plasma ignition delay, plasma instability, hefty power loss outside of the plasma, and RF interferences with other electronic instruments wired into the system. Even in manual mode, the ENI matching network

would become over-heated and 'jump away' during high-power operations. We eventually solved the problem by building a manual RF impedance matching network, similar in design to those used on EPV's large RF-PECVD manufacturing system. The home-made RF 'matchbox' has shown high efficiency of power-transfer into the plasma load and excellent stability under any conditions. For each deposition step, we monitor the plasma RF *current* which is a more pertinent gauge for plasma intensity than the commonly cited RF power (wattage).

The single junction solar cells are of the superstrate type: glass/$SnO_2$/p/i/n/Al, where the front contact is commercial grade $SnO_2$ on 3-mm thick soda-lime glass (mostly LOF TEC7 or AFG PV-TCO), which has relatively low transmission (< 79%) and low haze (< 6-7% near the red-color region) that adversely impact the short-circuit current, $J_{sc}$, of solar cells compared to higher quality TCO used by other groups. Most of the nc-Si:H i-layers (absorbers) were fabricated by RF-PECVD method using gas mixtures of silane ($SiH_4$) highly diluted by hydrogen ($H_2$). The advantages of our low-cost PECVD system include a large electrode utilization ratio (a single 12"x15" powered electrode is used to coat simultaneously *four* substrates equal to its size), high gas utilization, a controllable contamination profile, ease of operation, and low maintenance. Parallel processing (multiple substrates per powered-electrode) is effective in compensating for the rather low growth rates presently associated with device-quality nc-Si:H films. The substrate temperature was normally kept near 200 °C. Boron and phosphorus doped p-layers and n-layers were deposited in the same reactor as the i-layers, without *any* movement of the substrates and/or the reactor throughout the entire device fabrication. There was no reactor cleaning between the runs or between individual layers in a given run. After turbo-molecular pumping for several hours, the base vacuum typically reached the low-$10^{-6}$ torr range before the start of the nc-Si related deposition processes. A thin a-SiC:H p-layer was first deposited on the $SnO_2$. This was followed by a seeding procedure (which might comprise several steps) to induce crystallization for the Si:H i-layer (see Sec.3). Finally, an a-Si:H n-layer was grown. Sputtered Al was the standard back contact during this period, and ZnO/Al (not optimized) was occasionally used for comparison. Small area solar cells, near 0.2 $cm^2$ in size, were defined either by shadow masks during Al sputtering, or by etch-patterning after Al deposition. Light current-voltage curve (I-V), dark I-V, and spectral response (QE) were obtained for the solar cells. Device stability was studied under one-sun and 47-sun irradiances, and in the dark. Microstructures of the devices were probed by Raman scattering, X-ray diffraction (XRD), and atomic force microscopy (AFM) at NJIT. The optical absorption spectra of the nc-Si i-layers of a few devices have been studied by the infrared photocurrent spectroscopy technique at Syracuse University to be detailed later.

To judge if the Si:H i-layer (absorber) in device configuration is amorphous or nanocrystalline (including mixed-phase film containing significant fraction of nanocrystalline phase), we have primarily relied on the long wavelength quantum efficiency (QE) or red-response, and the $V_{oc}$, of the solar cell. We have also regarded superior stability of a thick device upon light exposure as being indicative of a substantially nanocrystalline absorber (in differentiation with that of a-Si:H). Occasional micro-structural examination by Raman scattering would confirm the 'phase' of the absorber. We lack capability to probe Si:H i-layers in their growth direction, which may evolve continuously from the amorphous state to the mixed-phase state and then, finally, to the nanocrystalline phase in many samples. Note that, up to now, we have been mainly concerned about the *relative* changes of device parameters with deposition conditions, and not the absolute efficiencies of the devices. Thus, optical engineering of the devices (front TCO and back contacts) has been largely 'neglected' in Phase I.

## 2.2 The apparatus for combined HWCVD and PECVD at Syracuse University

The main task at SU under the present subcontract is to develop a novel deposition approach to nc-Si by, in a single reactor, simultaneously exploiting RF-PECVD and HWCVD (hot-wire) which traditionally have been applied separately and independently. In the last ten years, it has been established that HWCVD is a viable technique to prepare nc-Si and polycrystalline Si thin films with high growth rates at low temperatures. However, solar cells and thin film transistors fabricated by HWCVD often exhibit inferior performance than those produced by PECVD. We intend to combine the advantages of the two techniques. During Phase I at Syracuse University, we have i) finished modification of the existing RF-PECVD reactor to serve as a combined plasma and hot-wire CVD system; ii) prepared a-Si:H and likely nc-Si films by RF-PECVD; and iii) started observing interactions between $SiH_4$+$H_2$ plasma and hot-filament in initial film deposition trials by the hybrid CVD method.

### 2.2.1 Upgrading an RF-PECVD reactor to a combined plasma and HWCVD system

Professor Eric Schiff's group at Syracuse University (SU) has been engaged in a-Si:H thin film research for twenty years, mostly on transport and opto-electronic properties. There existed at SU an RF-PECVD system (from Plasma Technology Ltd of UK) capable of both deposition and etching. This reactor was used routinely until 1994, but only used occasionally as required until 1997. From 1997 to the start of this program, some instrumental problem developed in the reactor which had been mostly idle. In Phase I, we focused on developing equipment/hardware in order to have deposition and characterization capabilities for nc-Si materials and solar cells. In the first three months, we made: 1) PECVD system fully operational through hardware and process modifications; 2) deposition of metal contact by reactive evaporation.

The RF-PECVD system at SU had a standard, capacitively coupled planner power electrode in diode configuration. There is a provision to convert it to triode configuration. Deposition process is computer controlled, with substrate temperature ranging room temperature to 400$^{\circ}$C. A specific feature, which is different from standard PECVD reactor, is the Pyrex glass chamber instead of stainless steel. Chamber cleaning is easy with minimal contamination during materials and device fabrication. The Pyrex glass chamber can be easily replaced by aluminum chamber if any additional in-situ measurements have to be performed. The reactor is capable of depositing n- and p-type a-Si:H films and its alloys needed to fabricate p-i-n a-Si:H or nc-Si:H solar cells.

In our effort to develop combined plasma and hot-wire deposition system, we first calculated the complete power balance in hot-wire CVD reactor and found that a major portion of electrical power is consumed by the filament holder. From our experience and published reports [7,8], a major source of metallic contamination during HWCVD is the evaporation from filament holder and from the electrical connections between the filament and the current carrying wires. Metallic impurities drastically affect the lifetime of the photo-generated carriers in Si thin films. In order to prepare clean Si thin films, we have fabricated a filament holder using ceramic materials instead of conventional metals. The chemical composition of the ceramics used is Zirconium phosphate. As shown in **Figure 1**, the filament holder is made of two rectangular ceramics frames, mounted on four ceramic posts and spacers that allow for adjusting filament height, or the distance between the filament and substrates. The bottom frame and the top frame are called, respectively, base and filament support. It is also possible to 'tilt' the plane of the filament with respect to the incoming flux of process gases. The shape of the filament holder

was chosen to minimize the current required to maintain a given filament temperature (with minimal power loss to the filament holder, according to power balance calculation), and to avoid confinement of decomposed species and process gases. The filament holder, 10x10 $cm^2$ in size, can hold up to 12 segments of 10-cm wires, for a total wire length of 1.2 meter. We have selected 0.5-mm diameter tungsten wire as the catalyzer. The ceramic filament holder, built at SU, can sustain temperatures to 2750°C. It may be noted from figure 1 that the connections between the tungsten wire and electrical wires are made outside of the area of the ceramic frame where Si layers will be processed. This may help minimize metallic impurities which would otherwise get incorporated into nc-Si and poly-Si films during HWCVD. The problems of impurities and film inhomogeneity during hot-wire CVD processing often arise from the design and electrical connections of filament holder. We believe that some of the technical problems with HWCVD will not affect the combined plasma and hot-wire CVD. In order to understand the technical challenges in combined plasma and hot-wire deposition, we are using a single wire so as to introduce minimum perturbation to the plasma. The filament holder is placed on top of the grounded electrode (anode). The height of the ceramic posts is 2.5 cm, slightly less than the gap between the RF electrodes (2.54 cm). Electrical connections from a Variac and transformer to the hot-wire have been made, using a feed-through in the reaction chamber, with special wires capable of high temperature (200°C) operation and low current leakage in the plasma. An optical pyrometer is used to measure the temperature of the filament observable through the Pyrex wall. The RF power supply is attached to the top electrode. Process gases enter the reactor through the bottom electrode (showerhead type), and are decomposed by the hot filament as well as RF excitation in the combined plasma and hot-wire CVD.

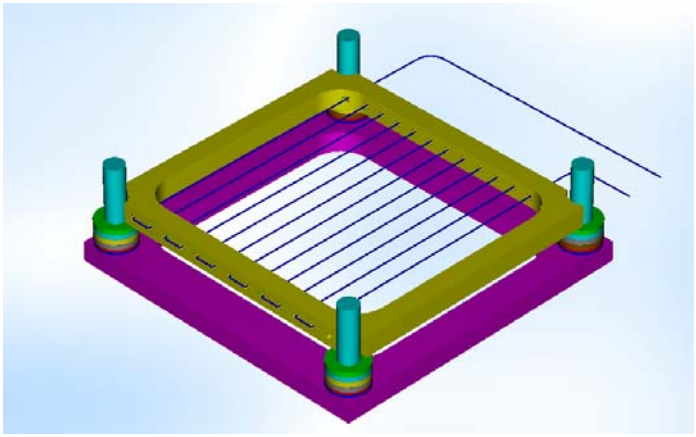

**Figure 1** Filament holder design for the combined HWCVD and PECVD system

Upon the completion of the 'combined' reactor, we created silane and hydrogen plasma and then turned on the filament. We observed an interesting effect, that the RF power and the $H_2$ to $SiH_4$ ratio (R) critically control the intensity of the glow discharge in combined plasma and hot-wire CVD. At high RF power (58 watt), $H_2$+$SiH_4$ plasma is turned off as soon as the filament is turned on. The plasma is visible again as soon as the filament is turned off. At low RF power (41.7 watt) and same dilution (R=20), plasma is again turned off when the filament is turned on. However, unlike higher-RF power case, the plasma does not return when the filament is turned

off. Interaction of hot-filament with plasma is also sensitive to high H-dilution, although under high dilution (R=20), plasma is turned off as soon as filament is 'ignited', whereas at low dilution (R=3.5) and the same RF power (58.5 Watt), plasma stays on when the filament is turned on, although the brightness of the plasma decreases. This phenomenon indicates that there is strong interaction between hot-filament and plasma. The electron-impact dissociation process somehow is strongly influenced by the state of the hot-filament. We are presently in the process of understanding the interaction between the $H_2$+$SiH_4$ plasma and the hot-filament, so that we can develop a qualitative model on the primary dissociation process in combined plasma and hot-wire CVD. Simultaneously, we are also trying to solve the technical problem associated with having stable combined plasma and hot-wire CVD process with wider process window.

### 2.2.2 Properties of Si:H films prepared by PECVD in the SU deposition system

As mentioned earlier, the RF plasma CVD reactor had not been functional since 1997. In the beginning of Phase I, we had to solve some technical problems to get it in working order. We then prepared a few a-Si:H and perhaps nc-Si thin films to verify that the RF-PECVD was restored to its original condition and capable of depositing high quality materials. The PECVD growth conditions and some preliminary properties of four Si:H films are described in **Table 1**.

| Sample No. | Type of Sample | Silane Flow (sccm) | $H_2$ Diln. | $P_r$ (mT) | RF Power (Watt) | $T_s$ (°C) | Cut off WLength (nm) | $\sigma_d$ ($Scm^{-1}$) | $\sigma_{ph}$ ($Scm^{-1}$) |
|---|---|---|---|---|---|---|---|---|---|
| 061002 | a-Si:H | 6.0 | 0 | 160 | 9.0 | 150 | 507 | $4.10x10^{-9}$ | $2.50x10^{-6}$ |
| 073002 | a-Si:H | 4.7 | 0 | 125 | 8.2 | 200 | 503 | $2.58x10^{-8}$ | $1.24x10^{-7}$ |
| 071602 | nc-Si? | 0.8 | 20:1 | 477 | 32.3 | 250 | 487 | $7.75x10^{-9}$ | $3.20x10^{-8}$ |
| 073102 | nc-Si? | 0.3 | 100:1 | 730 | 23.4 | 250 | 476 | $3.61x10^{-7}$ | $1.13x10^{-8}$ |

**Table 1** PECVD conditions, optical and transport properties of Si:H films from SU

Sample 061002 is amorphous having a dark conductivity ($\sigma_d$) and a photoconductivity ($\sigma_{ph}$) of $4.1x10^{-9}$ $Scm^{-1}$ and $2.5x10^{-6}$ $Scm^{-1}$, respectively. The $\sigma_{ph}$ was measured with a monochromatic light of 670 nm from a laser source at a power density < 5 mW. The $\sigma_{ph}$ of the sample 061002 appears to be high for 670 nm illumination, which can be attributed to its relatively high dark conductivity (~ $10^{-9}$ $Scm^{-1}$). The optical transmission spectra of the samples were measured by an UV-VIS spectrophotometer. The cut-off wavelength (T ~ 0%) gives a rough indication of the bandgap of the sample. The cut-off wavelength for sample 061002 is 507 nm which is in the range of standard a-Si:H films having comparable thickness. Although sample 073002 was prepared with pure $SiH_4$, its $\sigma_d$, $\sigma_{ph}$, and photosensitivity ($\sigma_{ph}/\sigma_d$ ratio) are not typical for a-Si:H for unknown reasons. Sample 073002 was deposited with pure $SiH_4$ at very low flow rate (4.7 sccm) leading to long residence time of $SiH_4$ inside the reactor. This in turn might have enhanced $SiH_4$ decomposition into silicon related radicals and atomic hydrogen (H). Samples 071602 and 073102 were deposited with high hydrogen dilution (R=20 and 100), so that the samples might have evolved to become nc-Si. Indeed, the $\sigma_d$, $\sigma_{ph}$, and $\sigma_{ph}/\sigma_d$ values indicate that sample 073102 is probably (at least partially) nanocrystalline. The cut-off wavelength of sample 073102, at 476 nm, is notably lower than that of sample 061002. This may be taken as another

indication of the presence the nanocrystalline phase. The value of $\sigma_d$ for the sample 073102 increases to $3.61 \times 10^{-7}$ $Scm^{-1}$, and both $\sigma_{ph}$ and $\sigma_{ph}/\sigma_d$ decrease compared to that of the sample 071602. The deterioration of electronic properties may be attributable to the higher chamber pressure (730 mtorr) used for growing sample 073102. X-ray diffraction or Raman study would be required to determine to what extent these films have developed into the nanocrystalline state.

### 2.3 Collaborations between EPV and Syracuse University

The present NREL subcontract requires close, continuous interaction between EPV and Syracuse University (SU) to exploit our complementary expertise and experience. In Phase I, a number of collaborative activities took place. Professor A.R. Middya of SU attended the 2nd International Conference on Cat-CVD (Hot-wire CVD) Process held on September 10-13, 2002 in Denver. He later summarized and reported the important results of the conference to the technical team at EPV. A one-day strategy meeting between the scientific staff of EPV and SU was held on the 20th of November, 2002, at EPV. During the meeting, A.R. Middya made a presentation on recent advances of nc-Si:H solar cells fabricated by RF-PECVD and hot-wire CVD. An in-depth discussion based on the talk was stimulating and productive. We planned research activities and identified characterization methods that would be effective for evaluating nc-Si materials and especially solar cells. A set of nc-Si single junction solar cells from EPV have been measured at SU by the Infrared Photocurrent Spectroscopy method (see Section 5.3). Numerous discussions took place on the IPS technique and data interpretation. More exchanges of samples and ideas are expected as SU starts to prepare nc-Si films by the combined plasma + hot-wire CVD method, and as EPV makes solar cells under varying conditions for seeding and for the nc-Si absorbers.

## 3.0 Seeding Methods for nc-Si Absorber Growth

The performance of nc-Si solar cells depends on many processing details, chief among which are the seeding/nucleation technique to be discussed in this section, and the growth conditions for the bulk of the nc-Si:H i-layers to be described in Section 4. Here seeding refers to the 'phase transformation' process from the initial amorphous-Si base-layer to the desired nanocrystalline-Si i-layer. This seeding step was found to be essential, regardless of deposition conditions for the 'bulk' Si:H i-layer, to ensure rapid yet device-friendly amorphous-to-nc transition. The plasma conditions in the nucleation stage need to be substantially different from those for the bulk nc-Si i-layer. More than half of the device runs conducted in Phase I at EPV (> 200) were devoted explicitly to the study of seeding effects on nc-Si single junction solar cell performance and absorber layer properties. One ought to clearly recognize that our seeding procedure is severely constrained by two critical considerations unique to EPV's approach: 1) The use of $SnO_2$ front contact preludes the possibility of growing nc-Si seed layer *directly* on the substrate (as $SnO_2$ is unstable against highly energetic hydrogen-rich plasma), requiring the presence of a 'protective' layer on $SnO_2$ that introduces notable optical loss; 2) Most importantly, in our *single*-reactor, single-chamber equipment, the seeding method must satisfy the stringent *non-contamination* requirement for nc-Si i-layer growth following the seeding procedure. The second demand is especially difficult to meet when high-intensity plasma is used for seeding (to be further discussed in Section 4). The use of $SnO_2$ as the front contact (versus commonly used ZnO) has proved to be highly challenging in terms of balancing seed layer efficacy and its optical transparency which must be kept high to ensure optimal photoresponse from the absorber.

### 3.1 A choice for nucleation: i-seeding instead of p-seeding

One of the main lessons we learnt in Phase I can be put in this way: the seeding process for nc-Si absorber can 'make or break' the nc-Si solar cell. Device optimization for nc-Si is much more complicated than that for a-Si:H because, in part, the quality or suitability of the deposition conditions for the bulk i-layer can *only* be evaluated in the context of a chosen seeding recipe, as seeding determines both the critical p/i interface and the evolving properties of the bulk i-layer. Simply put, *both* seeding and nc-Si absorber ('bulk' i-layer) have to be done 'right' (with compatible interface) in order for the device to work well. In contrast, the p & i layers in a-Si:H solar cells can largely be independently optimized. The a-Si:H solar cell consists of the same type of layers (amorphous Si and its alloys), while the nc-Si solar cells contain different types of Si:H films that must make abrupt yet smooth 'phase' transition. The strong interplay between the seeding process and the bulk i-layer growth is one of the major difficulties in obtaining, and reproducing, high performance nc-Si solar cells. We have established that, for a fixed set of i-layer plasma conditions capable of *sustaining* nc-Si growth, the seeding or incubation procedure (which may comprise several individual steps) largely determines the properties of the Si:H absorber, and *strongly* influences its device performance. Under the same Si:H i-layer growth conditions using moderately high RF power and high $H_2/SiH_4$ dilution, amorphous, mixed-phase, or nanocrystalline absorbers can be obtained, respectively, depending on the seeding method. **Figure 2** shows three distinctive Raman scattering spectra of three Si:H devices prepared with different seeding procedures but under the same i-layer plasma conditions. The strength of Raman signal near 520 $cm^{-1}$ is taken as a measure of nanocrystallinity of the Si:H absorber. For the sample made with poor seeding technique, evidence of nanocrystallinity was largely absent despite the long deposition time (~3 hours), as we had found in a number of the earliest devices.

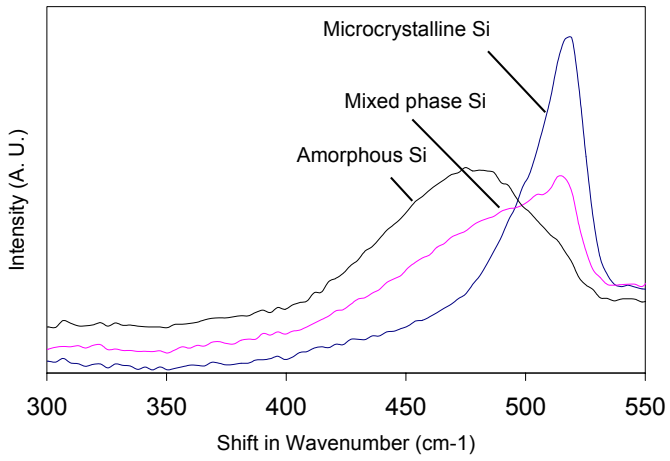


**Figure 2** Raman spectra of three Si:H solar cells prepared with different seeding methods

In Phase I, we extensively explored various 'seeding' schemes that might induce nc-Si growth on a-Si:H or a-SiC:H base-layers with minimal amorphous-to-nanocrystalline transition layer. Here we broadly classify the various seeding schemes into two categories: 1) *i-seeding*, which is to induce nucleation inside i-layer (close to the p/i interface), i.e., the 'phase transition' occurs inside the PV-active absorber itself; 2) *p-seeding*, which is to generate seeding action inside p-

layer (on the boron-doped p side of the p/i interface). In either type of seeding, very high $H_2/SiH_4$ dilution ratio, R, and high RF power tend to facilitate nucleation. To limit the thickness of the seed layer, a hydrogen-plasma etching step (which causes subtraction of film thickness) has sometimes been effectively used as a precursor to seeding layer growth (addition of film).

The i-seeding tactic is not widely practiced (we have not seen any discussion on this subject), presumably due to its poor device suitability resulting from the inevitable generation of high levels of defects by the energetic, strongly etching plasma needed for speedy nucleation in the seeding layer (which becomes part of the PV-active absorber). On the other hand, the motivation for studying i-seeding includes its relative suitability for single-chamber systems (where minimal deposition of doped layers is preferred), the absence of optical loss to 'dead' p-seed layer (as it is very tricky to grow transparent p-seed layer on $SnO_2$). We also speculated on the potential for higher $V_{oc}$ when a wider-bandgap a-Si:H 'buffer' layer was deposited on the a-SiC:H p-layer prior to the onset of the i-seeding process. Most importantly, given our single-reactor PECVD, i-seeding is believed to be more compatible with the low cross-contamination requirement as it can lessen the release of dopants (by high-power plasma etching) from pre-existing doped layers on some interior surfaces of the reactor during seeding processes before nc-Si i-layer deposition, and it minimizes the presence (the duration of use) of dopants. The cross-contamination issue is further described in Section 4. Early in Phase I, we deliberately chose to work on the higher risk, poorly studied i-seeding methods, instead of p-seeding. We have found that the relatively short i-seeding (a small fraction of the total i-layer deposition time) often has an even greater influence on device performance than that of the commonly used p-seeding.

To avoid p/i interface plasma damages, typically a thin undoped a-Si:H buffer layer (100–400 Å) would be first grown on the a-SiC:H p-layer, before the start of i-seeding and nc-Si:H absorber deposition. Two varieties of i-seeding were evaluated early on. In the simplest form, nucleation was attempted by intense glow-discharge etching, using pure $H_2$ feed-gas, on the a-Si:H buffer layer (resulting in a reduction of buffer layer thickness). This method did not work as the solar cells were either amorphous, or had terrible FF (e.g., 20-30%). We concluded that pure hydrogen etching, by itself, is incapable of producing a good 'template' for instantaneous nc-Si growth required for solar cell application. The poor device behavior was partially due to excessive plasma damages on the a-Si:H buffer layer as confirmed by poor device characteristics of a-Si:H control cells deposited on the etched buffer layer. The other, more effective i-seeding method was to deposit a thin Si:H 'incubation' film at very low growth rate from a $H_2$+$SiH_4$ gas mixture of extremely high R ($H_2$ to $SiH_4$ dilution ratio), followed by an optional step of grading of $SiH_4$ flow rate (while keeping $H_2$ flow rate constant) leading to the growth of 'bulk' nc-Si i-layer. The combination of H-plasma etching and subsequent $SiH_4$ grading (at the beginning of i-layer deposition) has proved to work much better than H-plasma etching alone. Still the solar cells obtained from the 'seeding and grading' method all had low FF (< 50%), weak red-light response, and sometimes rather high $V_{oc}$ (indicating that the initial i-layer was still mainly amorphous). The $SiH_4$ flow-rate grading step, seemingly beneficial in some cases, might be unnecessary if the seeding layers were sufficiently developed (closer to nc-phase), as evidenced from a number of experiments using either i-seeding or p-seeding. When marginal 'seed' layers are used, i-layer grading may help to complete the nucleation process. For now, we cannot rule out the utility of i-layer grading, especially as part of an overall seeding formula.

In **Table 2** we tabulate the PV parameters of some representative nc-Si single junction solar cells produced in Phase I using different seeding techniques, with a few variations in other device

aspects as indicated. The devices presented in the table have nc-Si i-layer thickness in the range of 1-2 μm (near 1.5 μm for most of the p-seeding samples with a deposition rate at ~ 1.2 Å/sec). The first two entries in the table illustrate PV properties of representative nc-Si solar cells made by the 'i-seeding + $SiH_4$-grading' method. It can be seen that i-seeding is capable of slightly higher $V_{oc}$ than that commonly attained from p-seeding. However all the devices made with this type of seeding showed low FF, low $J_{sc}$ with strong bias-dependence of the QE, and often notable light-induced degradation in efficiency. It is suspected that the absorbers in some of the devices were initially amorphous, becoming nanocrystalline only after certain film growth. A difficulty with interpreting data from the earlier nc-Si devices is that, at the time, both seeding and i-layer growth conditions were being varied, so bad i-seeding might not be the sole cause for bad device.

More recently, we attempted to improve i-seeding again after we had gained a lot more insights from studying p-seeding techniques (to be discussed in the next subsection). We have modified our earlier 'seed and grade' method to better take care of the interfaces. The degree of seeding must be carefully controlled, as 'over-seeding' inside i-layer can do more harm to the device than 'under-seeding'. Better FF has been observed with the modified i-seeding (vs. earlier i-seeding recipes), as exemplified by the two samples, R252 and R247, in table 2 (the third and fourth entries), which were prepared by a single i-seeding step without grading. The nc-Si i-layers in run #R247 and #R252 were deposited under the same conditions as all other p-seeding samples in table 2 (except #R130). Despite the improvements in FF by the modified i-seeding approach over those of all the previous i-seeding produced nc-Si solar cells, the short-circuit current density, $J_{sc}$, is generally still disappointing. The poor blue and low peak QE values, even under reverse electrical bias, put a major drag on conversion efficiency. In this case, the low $J_{sc}$ is not mainly caused by optical loss in the a-SiC p-layer, but is suspected to arise from carrier loss or recombination near the seeding interface (inside or close to the i-incubation layer), since the red-light QEs of such solar cells are relatively healthy and only weakly dependent on electrical bias.

| Run # | Type of seeding, other descriptions | $V_{oc}$ | $J_{sc}$ | FF | Effi. |
|---|---|---|---|---|---|
| | (seeding method, bulk i-layer feature) | (V) | ($mA/cm^2$) | (%) | (%) |
| R139-1 | i-seeding (on thin a-Si:H buffer over a-SiC p-layer) | 0.51 | 14.0 | 50 | 3.6 |
| R141-1 | i-seeding (on thin a-Si:H buffer over a-SiC p-layer) | 0.52 | 14.7 | 47 | 3.6 |
| R252-1 | i-seeding at moderate power, modified recipe | 0.46 | 15.1 | 59 | 4.1 |
| R247-1 | i-seeding at higher RF power, modified recipe | 0.46 | 15.2 | 64 | 4.5 |
| R140-1 | Thick p-seeding layer (over $SnO_2$/a-SiC p) | 0.50 | 13.8 | 70 | 4.8 |
| R130-1 | p-seeding; higher RF power for i-layer | 0.50 | 15.0 | 57 | 4.3 |
| R145-3 | p-seeding; some carbon added in seed layer | 0.49 | 13.2 | 68 | 4.4 |
| R147-3 | p-seeding, thinner a-SiC p & thinner seed layer | 0.50 | 14.7 | 65 | 4.8 |
| R175-1 | p-seeding with special pre-dep chamber cleaning | 0.50 | 15.5 | 65 | 5.0 |
| R144-1 | p-layer seeding; i-bulk grown @ higher rate (3Å/s) | 0.48 | 13.7 | 62 | 4.1 |
| R224-1 | p-seeding; Asahi $SnO_2$ front; ZnO/Al back contact | 0.49 | 17.6 | 62 | 5.3 |

**Table 2** Properties of selected nc-Si:H devices made by various seeding methods (with Al back contact except R224-1 made on special Asahi $SnO_2$ with ZnO/Al back contact)

We note that the various i-seeding processes have by no means been 'optimized', but in later part of Phase I, we decided to focus our limited resources on the more conventional p-seeding.

Although we have not made, by i-seeding techniques, nc-Si devices that are as efficient as those obtained by p-seeding (see below), the experiences we gained from studying i-seeding has proved to be valuable in our subsequent extensive investigation of p-seeding techniques.

### 3.2 p-seeding experiments and device optimization

Good nc-Si solar cells have been (relatively) easier to obtain by using 'nanocrystalline' p-layers as templates for the subsequent formation of nc-Si i-layers. The obvious advantage of creating 'seeds' inside p-layer (p-seeding) is that, when the amorphous to nanocrystalline 'phase transition' occurs in the 'dead' p-layer instead of the PV-active i-layer (as is the case with i-seeding), high density of defects associated with incubation layer (amorphous and early-stage mixed-phase material) can be avoided on the absorber (i-layer) side of the critical p/i interface, thus the entire i-layer can be made nanocrystalline for good solar cell function. The inadequate performance of i-seeding in our early experiments led us to more aggressively pursue the p-seeding strategy (used by all other groups working on p-i-n type nc-Si solar cells) since the mid-point of 2nd quarter of Phase I. (Of course, as stated before, it is highly unlikely that the full device potential of i-seeding has been reached after the rather limited efforts.) The process window is wider for p-seeding as since there is little need to guard against defect creation or contamination of p-layer. For instance, more energetic plasmas can be used for faster nucleation action. Hydrogen-plasma 'etching' alone on the p-layer appeared to be capable of inducing nc-Si absorber growth when high RF power (compared to that used for i-seeding) was applied for an extended period. However, after a number of trials, we concluded that etching alone did not provide adequate seeding for growing good nc-Si absorber. The deposition of a nc-Si p-layer (probably not truly nanocrystalline) on top of the a-SiC p-layer was found to be a much more preferable p-seeding method. The seeding p-layer would be grown either directly on the a-SiC:H p-layer, or deposited after a H-plasma etching step on the a-SiC:H p-layer. This 'nc-Si p' seeding technique has led to solar cells of superior FF, good carrier collection, better seeding uniformity, and improved reproducibility of the solar cells. The major problem that we have been working on, with quite limited success, is the low $J_{sc}$ brought about by significant optical loss to the optically-opaque p-seed layer. Some examples of p-seeding produced solar cells are given in Table 2 above. Conversion efficiencies of ~5% have been obtained on commercial $SnO_2$ with Al back contact for several runs, an example of which is seen in **Figure 3**.

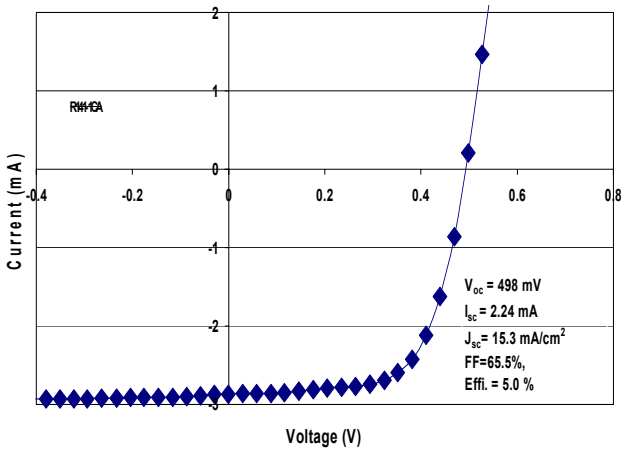


**Figure 3** I-V of a nc-Si:H single junction solar cell made by p-seeding

In addition to p-seed layer absorption, the low $J_{sc}$ values of the solar cells are attributable to optical losses to the front TCO contact and glass, low TCO texture, thick a-SiC:H p-layer (protective layer for $SnO_2$), and the lack of good rear reflector (Al). In many cases, poor carrier collection is suspected to further compromise the spectral response (particularly in the blue to green light region). In Phase I, only a few nc-Si devices made by p-seeding show reasonably good $J_{sc}$ (from both light I-V and QE tests), but unfortunately, as we later determined after a large number of failed attempts to reproduce devices of comparatively high $J_{sc}$ (and high efficiency), the efficacy of what appeared to be the most promising p-seeding recipe was highly dependent on the operating history of the single-reactor, single-chamber system. Apparently, in a single-reactor system that has accumulated doped layers from earlier deposition runs, strong plasma excitation can result in dopant contamination of the reactor during the seeding process even if the feed-gas mixture for the seeding plasma does not contain dopants.

With p-seeding, we routinely obtain FF in the mid-60% range. However, the $V_{oc}$ of the cells has been inconsistent, with typical values in the 440-470 mV range for the more recent runs. It is unclear how we can increase the $V_{oc}$ without degrading FF and/or $J_{sc}$. The $V_{oc}$ seems to be higher for devices on smoother $SnO_2$ TCO. Our earlier solar cells made with p-seeding exhibited good $V_{oc}$ near 500 mV (see table 2), but such devices were not satisfactorily reproduced in later runs, even after we had better control over cross contamination and process gas purity issues. Low $V_{oc}$ may result from some kind of 'mismatch' between the seeding layer and the i-layer. For a given type of seeding, lower $V_{oc}$ is normally found in cells with higher degree of i-layer nanocrystallinity (see next section). Thus, it would appear that higher $V_{oc}$ can be obtained if the initial i-layer is almost mixed-phase (*not* highly nanocrystalline). We are continuing to address the $V_{oc}$ problem in Phase II of this subcontract.

In a few tests with ZnO/Al back contacts replacing the standard Al contacts, higher $J_{sc}$ values were obtained. So far, the sputtered ZnO has not been optimized for higher efficiency (due to contact barrier between the a-Si n-layer and ZnO), but its absorption-enhancement effect on the solar cells has been evident. Sample R224 was made with Asahi 'U' $SnO_2$ (recipe not adjusted) which contributed to an increase of $J_{sc}$ (by > 1 $mA/cm^2$). From the two runs of nc-Si solar cells made on Asahi $SnO_2$, the FF values were actually lower (but the $J_{sc}$ and $V_{oc}$ are higher) than those of solar cells made on the default TCO (commercial $SnO_2$ such as LOF TEC7). As pointed out by a number of publications, the seeding process (phase evolution) depends on the morphology of the underlayer. Given the higher haze (more texture) of the Asahi 'U' type $SnO_2$, it is perhaps not surprising that the seeding recipe needs to be re-tuned to get the same or better performance (FF) as that obtained on the smoother, lower haze (lower red-response) LOF $SnO_2$.

We also observed an effect of carbon concentration in the a-SiC:H p-layer on nc-Si:H devices produced with one version of p-seeding techniques. Recall that the a-SiC:H p-layer was grown on $SnO_2$, prior to seeding, mainly to prevent $SnO_2$ reduction by hydrogen-rich plasma. Higher $CH_4$ gas flow during a-SiC:H p-layer deposition apparently could degrade the potency of the subsequent seeding process. As an example, **Table 3** lists the PV parameters of two nc-Si solar cells prepared with different $CH_4$ volume fractions in the gas mixtures for the a-SiC:H p-layer depositions. It would seem that carbon species incorporated into the base-layer can influence the seeding process (which does not explicitly involve carbon), or somehow carbon (methyl groups?) can be 'released', from somewhere in the reactor, by strong plasma 'agitation'.

| Run # | Descriptions | $V_{oc}$ | $J_{sc}$ | FF | Effi. |
|---|---|---|---|---|---|
| R203-1 | High $CH_4$% in gas mixture for a-SiC:H p-layer | 0.46 | 14.3 | 59 | 3.9 |
| R205-1 | Low $CH_4$% in gas mixture for a-SiC:H p-layer | 0.48 | 14.5 | 63 | 4.4 |

**Table 3** Two nc-Si solar cells made with different carbon contents in a-SiC:H p-layers

We have also made preliminary attempts at creating nc-Si*C*:H p-layer as the seed layer by adding some $CH_4$ to the normal gas mixture of $H_2$+$SiH_4$+TMB during p-seeding deposition. At low $CH_4$ concentrations (in the feed gas mixture), no major difference was observed between devices made by Si:H and SiC:H seed-layers, except that $J_{sc}$ was slightly higher in the case of SiC:H seed layer (from higher short-wavelength QE) compared to seeding without carbon. The $J_{sc}$ was still low (< 14 mA/cm$^2$) even in these SiC-seeded devices. Generally, the p-type seed layers behaved like thick, narrow-bandgap (opaque) films. The use of higher $CH_4$ flow rate during p-seeding resulted in an much inferior device, suggesting the loss of seeding efficacy caused by excessive incorporation of carbon in the seed layer. We have not further pursued p-type nc-SiC seed layer in the latter half of Phase I due to the overriding need to first secure a simpler baseline p-seeding process without the complication of carbon alloying.

**Figure 4** shows an example of the impact of seeding procedure on the spectral response (QE) of nc-Si:H single junction solar cells. The i-seeding processes described earlier (creating 'seeds' inside and near the beginning of i-layer) have often led to higher blue and peak QE compared to p-seeding (nucleating on the p-layer side of the p/i interface). As stated before, i-seeding typically leads to better $J_{sc}$ (QE current) but lower solar cell efficiency compared to p-seeding, apparently due to poor photocarrier extraction under PV operating conditions (inferior FF). Only a few p-seeding solar cells have shown reasonably good QE-derived currents and high efficiency at the same time (using a special p-seeding recipe of unsatisfactory reproducibility). Thus far, all the nc-Si solar cells made with several better-reproduced p-seeding recipes (with the common feature of using a thick 'nc-Si' p-layer) have shown greatly suppressed QE (notably low short wavelengths and peak responses), as illustrated by the QE of the 'thicker p' sample in figure 4.

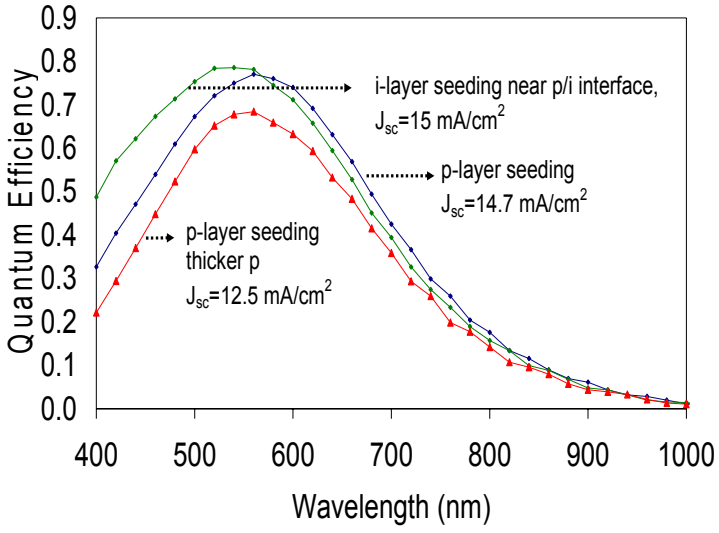


**Figure 4** Effect of seeding on QE spectra of nc-Si:H solar cells

The time required for adequate seeding obviously depends on the intensity of the plasma (among other things) that dictates the interaction and exchange between atomic hydrogen and Si species. Stronger plasma induces faster nucleation, often at the cost of worse seed-layer uniformity. The symptoms of insufficient seeding may include poor FF and high $V_{oc}$. However, FF and $V_{oc}$ do not necessarily vary, beyond a certain threshold, with increasing length of seeding. That is, longer (or further developed) seeding does not ensure a better FF or a markedly different $V_{oc}$, while the $J_{sc}$ tends to decrease with increasing duration of p-seeding. As an example, **Figure 5** displays the variations of solar cell parameters FF & efficiency (a), and $J_{sc}$ & $V_{oc}$ (b), of a series of solar cells fabricated with increasing seeding time, under a fixed set of p-seeding conditions using a mixture of $H_2$+$SiH_4$+TBM. All the other processing steps were kept the same for the series. When the seeding time was too short or the device was under-seeded, FF and efficiency were quite low as we have seen plenty of times. Seeding time much longer than some critical point (~400-450 seconds in this particular case) led to reduced $J_{sc}$ and lower conversion efficiency compared to that of the device with an 'optimal' seeding time. A crucial question that remains to be answered is this: Does the p-seed layer have to reach some *minimum thickness* before it is 'crystallized' enough to act as an effective template for the ensuing nc-Si absorber? If certain thickness has to be reached for p-seed layer, significant optical loss will be inevitable.

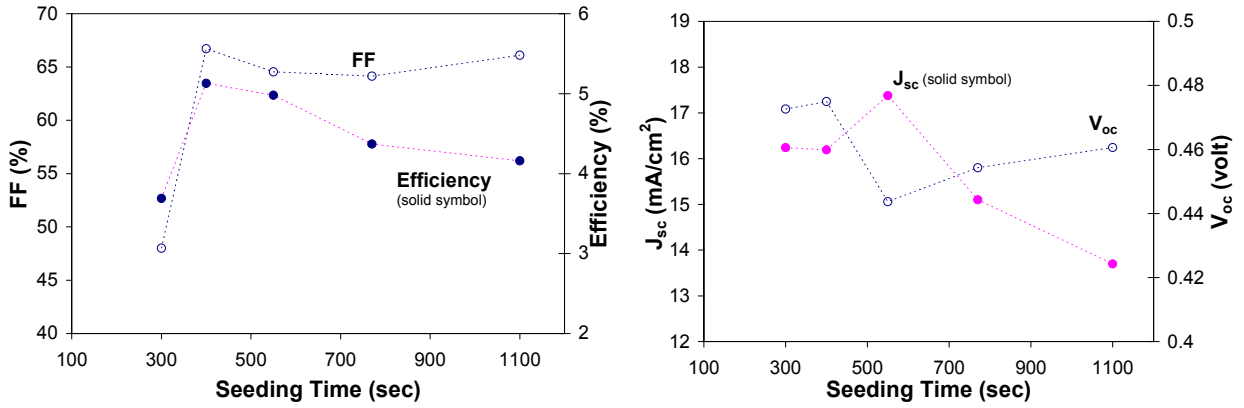


(a) (b)

**Figure 5** Variations of FF & efficiency (a), and $J_{sc}$ & $V_{oc}$ (b), with p-seeding time

## 3.3 Summary of observations on seeding

Much work remains to be done in the vital area of seeding, not only for single junction nc-Si solar cells, but more importantly for the bottom cell of a-Si/nc-Si tandem devices that we have begun to study. The following serves as a summary of our findings on the subject of seeding:

- Seeding has a bigger impact on nc-Si device performance than i-layer deposition conditions. The properties of Si:H absorber layer (especially the initial part) depends on seeding.
- Both p-seeding and i-seeding are capable of producing good nc-Si devices, but apparently it is easier to arrive at a good working recipe using p-seeding.

- It is possible to fabricate good p-seeded p-i-n type devices on plain $SnO_2$ (in contrast to the commonly used ZnO). However, the use of $SnO_2$ as front contact, and the needed precaution against single-chamber cross contamination, seriously impair the optimization of seeding.
- Low $J_{sc}$ remains the biggest issue with our present p-seeding techniques. So far, the more robust p-seeding recipes are accompanied by unacceptably high optical loss.
- The reproducibility of i-seeding appears to be better than some versions of p-seeding. There is promise of lower contamination by i-seeding for our single-reactor system.
- The efficacy of seeding depends on the properties of under-layers (carbon%, TCO texture).
- Interface i-layer grading may not be necessary when seeding is done 'right'.

# 4.0 Properties of nc-Si i-layers, Contamination, and Process Control

## 4.1 An exploratory survey of nc-Si i-layer growth conditions

Compared to the emphasis we have placed on the critical seeding processes, nc-Si i-layer deposition conditions have not been examined nearly as extensively or fruitfully. A reason for this relative 'neglect' of the i-layer is that, seed layer and i-layer must *both* work well to get a good solar cell. The study of 'undoped' nc-Si film in device configuration is feasible only after the establishment of a fairly robust, effective seeding technique. In the 2nd half of Phase I, a fixed set of conditions were somewhat arbitrarily chosen for the deposition of all the nc-Si i-layers as we focused entirely on p-seeding techniques, device reproducibility (contamination and process control), and tunnel junction aimed at a-Si/nc-Si dual-junction solar cells.

In the first half of Phase I, we cursorily surveyed the PECVD parameter space for conditions that are compatible with steady, sustainable plasma of $H_2$ + $SiH_4$ (+ Ar) gas mixtures which have been typically employed in the growth of nc-Si:H as reported in the literature. Important plasma parameters under study included RF power (plasma current), R ($R=H_2/SiH_4$ flow ratio), total gas flow rate, and chamber pressure. Addition of small amounts of Ar to the $H_2$ + $SiH_4$ mixture was only briefly tested (without clear benefit). The impurity contents of the i-layers have not been determined. Glow-discharge plasma could not be ignited and/or sustained for $H_2$-rich mixtures of $H_2$ + $SiH_4$ (e.g., when R=20) at low pressures (for instance, < 0.6 torr). This may be due, in part, to the relatively narrow spacing between the electrodes (separated by the two substrates that are placed on the surfaces of the opposing electrodes). Adding significant amount of Ar to the supply-gas mixture helps attain and maintain RF plasma at lower pressure and/or lower RF power. For deposition rate purpose, we have been mainly interested in moderate to relatively high chamber pressures (> 1.5 torr), using the high $H_2$ dilution (high R) approach to nc-Si growth. The thickness (and solar cell performance) uniformity of the deposited a-Si:H and nc-Si:H films over the 12"x15" substrates were routinely measured at selected positions. A general finding is that, under the conditions of high R (ranging from 40 to 250 for the bulk i-layer) and high RF power (> 150W using the home-made RF impedance matching network), the higher the chamber pressure, the worse the film and device non-uniformity, even in situations when $SiH_4$ depletion ratio is estimated to be < 50%. Such deposition inhomogeneity (see Section 5) is believed to result from strong plasma excitation (production of $SiH_x$ radicals) and relatively poor distribution (flow pattern over the surface areas of the substrates) of the source gas ($SiH_4$) molecules inside the RF-PECVD reactor. Improvements of nc-Si film deposition uniformity will be a vital undertaking for achieving future sub-module performance goals set in this subcontract. Due to

lack of material characterization capabilities at EPV, few stand-alone nc-Si films have been deposited on plain glass or other types of substrates.

As noted earlier, even though we made a good number of nc-Si absorbers using a variety of R and RF power under different pressures (many of the devices were made with i-seeding, and often with an initial i-grading) in the first half of Phase I, the qualities of the different nc-Si i-layers (in p-i-n devices) cannot be meaningfully compared to each other due to the substantial variations in the seeding methods used. Good devices must have high quality nc-Si absorbers, while the reverse is not necessarily true. The earlier 'shooting in the dark' efforts were intended to crudely elucidate some key concepts or promising approaches for nc-Si device fabrication, not to explicitly evaluate i-layer properties. As aforementioned, seeding is more influential than i-layer processing for device quality. In other words, a firm conclusion we have reached regarding i-layers relates to the importance of phase transformation, not the 'bulk' properties of the well-developed nc-Si. Via more developed seeding methods, nc-Si solar cells with reasonable FF have been deposited at higher than normal growth rates, using higher RF power that presumably causes higher defect density in nc-Si i-layer. An example is given by run #R144 in table 2 (see Section 3.2). Device uniformity became much worse at higher growth rates, not simply due to i-layer thickness variations, but rather the 'phase' property of the i-layer. Based on some data to be presented in Section 5, we conclude (and concur with numerous published reports) that the best nc-Si absorbers are made under plasma conditions close to the '*edge*' of the amorphous-to-nanocrystalline transition. In fact, a much higher degree of nanocrystallinity is, perhaps counter intuitively, detrimental to device performance (at least for all the nc-Si devices we have made). The understanding of this phenomenon, in our opinion, is infinitely more important than, say, the achievement of lower defect density in nc-Si i-layers. Some kind of grading or modulation in plasma parameters may be helpful for maintaining the 'near-edge' conditions over large areas and/or over long deposition periods. This will be a key subject for future study.

## 4.2 Contamination, device reproducibility, and process control

Dopant cross-contamination and gas impurity have severely hindered our efforts to effectively conduct experiments on fundamental device processes. Apart from these 'extrinsic' effects, we need to consider possible 'inherent' causes for the unacceptable performance variations in many ostensibly 'reproduced' nc-Si devices. One is the overall robustness of p-seeding layer (when using p-seeding technique), in terms of doping efficiency, thickness, and 'seed readiness'. Again, in a single reactor system, the above may depend on the recent operating history of the reactor. Also relevant is the compatibility of the seed layer (seeding surface) with the subsequent nc-Si i-layer. There are indications that excessive defects (related to harsh plasma conditions) on the seeded surface can degrade nc-Si (and a-Si:H) solar cell performance. Conceivably, p/i interface defects formed by aggressive seeding processes could limit both $V_{oc}$ and FF (and blue response). When an a-Si:H i-layer was grown on a 'seeding layer' (made with high power and long duration that would have resulted in immediate nc-Si growth if nc-Si i-layer conditions had been used), the resulting a-Si:H p/i/n single junction solar cells exhibited much lower $V_{oc}$ and FF compared to a-Si:H control cells deposited on standard a-SiC:H p-layers. Since the PECVD seeding process involves energetic etching plasma, we postulate that seeding should not be 'overdone'. There may exist an optimal balance between densities of 'seeds' and defects near the seeding surface. The delicacy of this balance could cause some difficulties with device reproducibility.

### 4.2.1 Phosphorus contamination of i-layers

We cannot overemphasize the difficulties in dealing with residual dopant cross-contamination of nc-Si 'i'-layers brought about by successive, alternate depositions of doped and 'undoped' layers in the same reactor in a single chamber system. Greater progress would have been made in understanding the nc-Si solar cell fabrication processes had we not been frustrated repeatedly by the lack of clear differentiation between contamination effects and true response of device performance to the designed changes in processing conditions. On the other hand, there really should be no surprise that contamination control is essential in a single-reactor environment as nc-Si is much more sensitive to background doping species (and to all sources of impurities) due to the much higher doping efficiency in nc-Si compared to that of a-Si:H.

The robustness of any seeding recipe must be judged in the context of its compatibility with low contamination requirement imposed by single-chamber PECVD. As noted earlier, some of the p-seeding recipes have been poorly reproduced and are sensitive to the single-reactor history of doped-layer depositions. In fact, the best nc-Si solar cells thus far were fabricated by p-seeding recipes suitable only if the reactor was relatively 'clean' (without n-layer deposition immediately prior to the present device deposition). The release of phosphorus from previously-deposited n-layers inside the reactor has been a chief suspect of poor reproducibility in some promising p-seeding recipes. This is particularly serious for some etching dominant p-seeding methods (when Si:H film is removed from the surfaces), as the highly energetic p-seeding plasma can 'liberate' dopants embedded in the doped layers shallowly buried below the surface of Si-film coatings. This mechanism of contamination is an important consideration in our recent efforts to attain better device reproducibility by developing tighter control over the p-seeding process, where the *growth* of p-type seeding film is much preferred than 'etching' dominated processes (involving removal of 'old layers'). That is, for contamination prevention, there should be net film addition (stronger growth than etching) over the plasma exposed surfaces during p-seeding process. Of course, the situation actually gets very tricky, as when there is too much p-seeding film deposited, optical loss becomes unacceptably high. We are still searching for a good trade-off between p-seeding effectiveness and optical transparency of the p-type seed layer.

Cross contamination of nc-Si i-layer by residual boron, and particularly by phosphorus, is an immense challenge for device process control and optimization with our single-chamber, non-load-locked system. Dopant species previously 'deposited' inside the reactor (within the same reactor cleaning cycle) can be released during and after intense plasma actions. Both seeding and i-layer growth (particularly the initial stage) can be adversely impacted. Reproducibility problem has seriously limited our choice of processing parameters. Tests indicate that boron contamination from p-layers (including p-seeding) is mild relative to that of phosphorus resulting from n-layer depositions using $PH_3$. The extent of nc-Si:H i-layer contamination seems to correlate with the amount of $PH_3$ used in the most recent n-layers, and the thickness and doping level of the p-layer immediately preceding the nc-Si:H i-layer. In the most severe cases of P-contamination due to excessive use of $PH_3$ in the formation of nc-Si n-layers (intended to form tunnel junctions in tandem devices), devices (nc-Si:H absorbers) became so conductive that dark I-V curves no longer resembled diode behavior. The level of residual phosphorus inside the chamber was undetectable by RGA. Some clues about P-contamination may be provided by the dependence of QE spectrum on *forward* electrical bias, normalized to the zero-bias QE (to obtain QE ratio spectra), as illustrated by **Figure 6**. Consistent with its low FF, the relative QE reduction of the phosphorus-contaminated solar cell from run #R193 is much more pronounced

compared to the 'uncontaminated' reference cell from run #R175, especially at the longer wavelengths (suggesting difficulty with photo-hole extraction), upon application of a moderate, forward electrical bias. As expected, the lightly boron-contaminated sample, R240, shows some weakness in its QE ratio spectrum in the short-wavelength region, but looks OK elsewhere. To suppress phosphorus contamination, we have developed n-layer processes with reduced $PH_3$ usage, and with better 'burial' procedure by the subsequent p-layer and/or p-seeding steps.

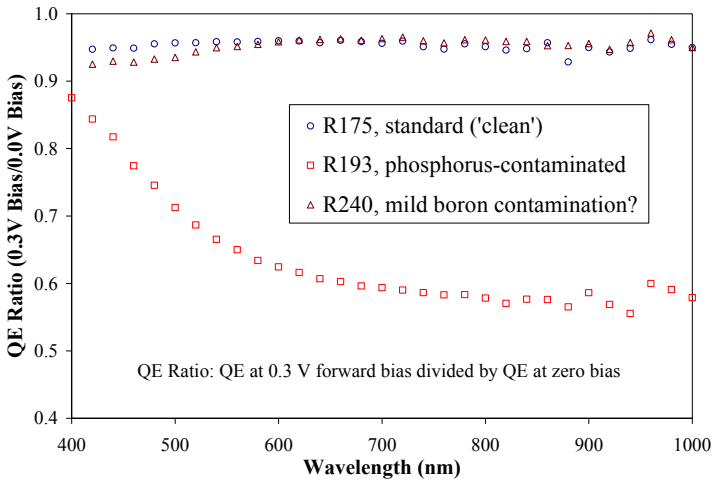


**Figure 6** Effects of dopant contamination on QE ratio spectra of three nc-Si:H solar cells

### 4.2.2 Purity of Process Gases

The impurity level of the process gas has also played a vital role in nc-Si:H device preparation. Due to the high R values during nc-Si i-layer deposition, purity of $H_2$ gas has been found to be far more influential than the base vacuum reading (which was typically near $2x10^{-6}$ torr) at the onset of i-layer deposition. Until late last year, we had not used oxygen getter (gas purifier) for nc-Si processes. Soon after the advent of some promising p-seeding recipes for nc-Si single junction cells, we experienced a major drop in device performance after the replacement of a nearly empty hydrogen gas cylinder (Cylinder I) with another cylinder (Cylinder II, from a different vendor). Even though the *nominal* purities of both cylinders were the same at six-nines (99.9999%), vastly different devices were produced using identical deposition recipes and procedures. The device non-uniformity distribution also changed, such that some previous mixed-phase areas turned into amorphous-Si after the $H_2$ cylinder change. **Figure 7** depicts the effects of $H_2$ gas purity on the QE spectra of three nc-Si:H solar cells prepared under otherwise identical conditions (within the same reactor-cleaning cycle). The highest QE (and efficiency) was obtained from the device made with the older, presumably cleaner $H_2$ from Cylinder I. The lowest QE came from a solar cell made with $H_2$ from Cylinder II. With the same 'bad' $H_2$ cylinder (II), a $H_2$-gas purifier was used to produce the solar cell with the intermediate QE in figure 7. The data interpretations for numerous nc-Si devices (showing poor reproducibility) were complicated by the use of $H_2$ gas of suspected lower purity. Some experiments indicate that even p-seeding can be sensitive to gas purity. This is rather surprising since p-seeding involves heavy boron doping, and low purity level should not matter. It is possible that when the seeding is not 'deep' (not well developed), gas impurities can compromise the seeds during or

after seeding plasma. We have taken measures to ensure the consistent use of high-purity gases. Note that good a-Si:H 'control' solar cells (FF > 73%) were made with all the $H_2$ gas cylinders. Presently, the purities of our $H_2$ and $SiH_4$ are respectively six-nines and five-nines (99.999%).

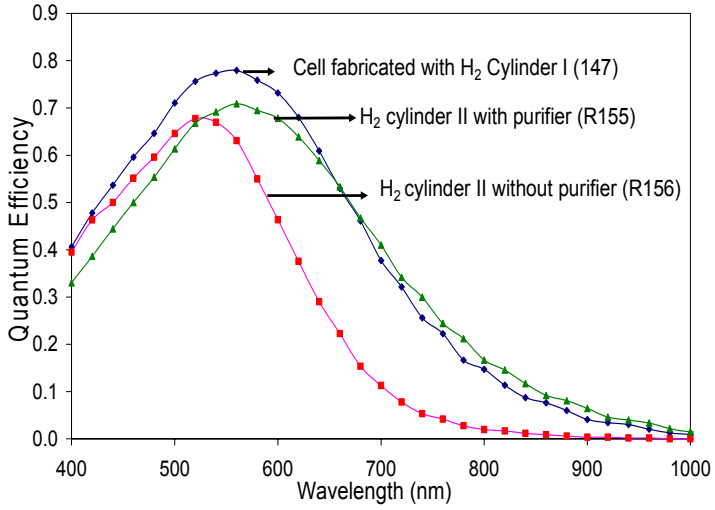


**Figure 7** Effects $H_2$ gas purity on QE of nc-Si:H solar cells

**Table 4** presents the properties of representative solar cells made with or without dopant or gas-impurity contamination. We have made a number of repeat runs for R175, with widely varying results. Some of these runs had P-contaminated i-layers. But even in cases where phosphorus contamination was carefully prevented, the device reproducibility was still rather unsatisfactory.

| Run # | Descriptions | $V_{oc}$ | $J_{sc}$ | FF | Effi. |
|---|---|---|---|---|---|
| | | (V) | (mA /cm$^2$) | (%) | (%) |
| R175-1 | A cell made with 99.999% $H_2$ with purifier | 0.49 | 13.8 | 65 | 4.4 |
| R186-1 | Same recipe as R175, but *contaminated* with P | 0.51 | 5.0 | 46 | 1.2 |
| R221-1 | 'Exact' repeat of R175, incl. reactor 'history' | 0.46 | 14.0 | 64 | 4.1 |
| R147-3 | A 'clean' sample, p-seeding (99.9999% $H_2$) | 0.50 | 14.7 | 65 | 4.8 |
| R210-1 | Same recipe as R147 above, with 99.999% $H_2$ | 0.45 | 14.0 | 63 | 4.0 |

**Table 4** Comparison of nc-Si solar cells from 'clean' runs and contaminated runs

In summary of section 4.2, cross contamination by phosphorus can only be kept to acceptable levels for nc-Si devices by imposing rigorous operational care and severe limitations on the operating parameters for dopant-related processes. The minimum gas purity necessary for nc-Si solar cell fabrication (in our system) remains to be seen. This will be studied at a later date when we have more confidence in a baseline recipe that is robust at least with high purity gases.

### 4.3 Stability of nc-Si:H single junction solar cells

A number of nc-Si single junction solar cells have been light soaked under one-sun or 47-sun (accelerated light soaking) conditions. Some of the earlier devices made with improper i-seeding

methods degraded severely (> 50%), as these cells appeared to have mixed-phase absorbers (high $V_{oc}$ and low red response). This is not unexpected considering the thickness of the i-layers (near 1.5 μm). The more recent, p-seeding prepared, relatively high efficiency solar cells with high red response and high FF have shown excellent stability. **Figure 8** shows the percentage change in efficiency of a nc-Si device under 47-sun illumination, along with that of an a-Si:H single junction solar cell (i-layer ~ 5500 Å). Good device stability has been confirmed, on selected nc-Si cells (> 4% efficiency), upon long-term exposure to one-sun illumination. We have not observed any significant post-deposition, air-exposure induced instability among the nc-Si solar cells. (Many of the earlier samples have been lost due to severe 'peeling off' of old AFG $SnO_2$ TCO from glass, a problem that seems to be under control with newer version of AFG $SnO_2$.)

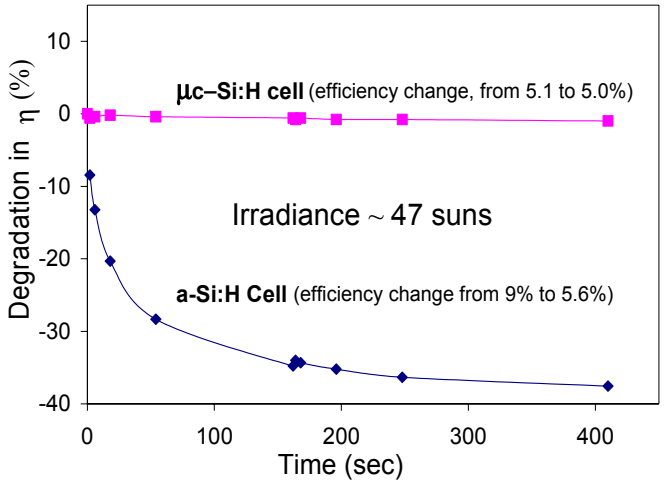


**Figure 8** Stability of a nc-Si:H and an a-Si:H single junction solar cell under intense light

## 4.4 nc-Si absorbers deposited from Ar + $SiH_4$ gas mixtures (argon dilution)

A number of attempts have been made to find out if Ar dilution alone, instead of hydrogen, of silane is a viable method for growing nc-Si i-layers for solar cell purposes. Note that previously we prepared a-Si:H solar cells, using substantial argon dilution of $SiH_4$ (with an Ar:$SiH_4$ dilution ratio up to 20:1), with superb initial performance. However, the *stability* of Ar-dilution prepared a-Si:H solar cells (upon light soaking) showed no improvement compared to that of solar cells prepared by the conventional hydrogen dilution method. One of the original motivations for studying Ar dilution for nc-Si was to find an alternative, non-etching plasma for p-seeding directly on the $SnO_2$ substrate (without the plasma 'damages' associated with hydrogen plasma). An argon-rich, non-etching plasma also helps to keep the single-reactor system clean by avoiding etching-induced release of contaminants often encountered with strong H-plasmas.

When Ar was used for both i-seeding and bulk i-layer growth with high Ar dilution (> 40:1) and moderate RF power, no signature of nanocrystallinity was detected by device QE or Raman scattering measurements. Apparently, Ar-rich plasma is not nearly as effective for seeding purposes as hydrogen plasma. Later on, to facilitate nucleation and promote crystallization, the Ar-dilution absorbers were grown on top of p-seeding layers which had been prepared by the

more familiar hydrogen-dilution methods. The hydrogen dilution seeding recipes were the same as used for making good nc-Si absorbers from $H_2$+$SiH_4$ gas mixtures (pure hydrogen dilution). That is, the initial seeding was done by hydrogen dilution, and the subsequent bulk Si:H absorber growth was carried out entirely with Ar dilution (Ar gas nominal purity = 99.9999%) in a hybrid approach. When higher RF power was applied to the Ar + $SiH_4$ mixtures, nc-Si:H absorbers were indeed obtained on hydrogen seeded surfaces. Selected samples from run #R165 and R166, in device configuration without the Al back contact, were examined by Raman scattering spectroscopy at New Jersey Institute of Technology. The Raman spectra indicate substantial degrees of nanocrystallization in the absorbers (i-layers) made purely by Ar dilution, as shown in **Figure 9** for some samples of R165 (from various positions over the 12"x15" plate).

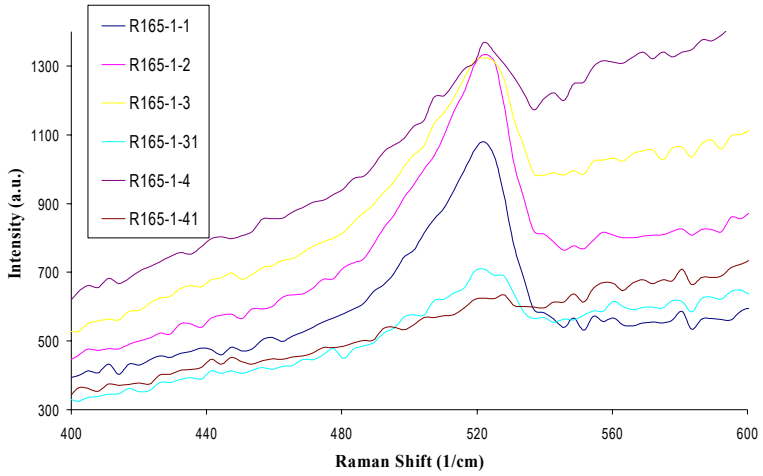


**Figure 9** Raman spectra of nc-Si cells made from Ar+$SiH_4$ mixtures by H-dilution seeding

The Ar-dilution produced nc-Si solar cells have exceedingly low efficiency (< 0.3%), with very low $V_{oc}$ (< 0.3 V), $J_{sc}$ (< 4 mA/cm$^2$), and FF (< 30%). Apparently, nc-Si i-layers derived from heavily Ar-diluted plasma are extremely defective, showing strong bias dependence of photo-carrier collection efficiency. (Similarly, a-Si:H cells made from Ar + $SiH_4$ mixtures with very high Ar dilution and/or at high RF power are also highly inefficient in PV performance.) Another serious issue with Ar dilution is the excessive film thickness non-uniformity when high Ar dilution ratio and high excitation power are applied (considerably worse than that of hydrogen dilution under similar dilution ratios, total gas flow rate, and RF power). The nc-Si devices made with highly energetic Ar-rich plasma are stable against air and light exposures. In view of the low efficiencies of Ar-dilution produced nc-Si solar cells, we do not plan to pursue this avenue, and shall be focused on hydrogen dilution (perhaps aided by supplementary Ar dilution).

## 5.0 Structural and Optical Characterization of nc-Si Absorbers

In this section, we report on the microstructural characterization and optical absorption spectra of the nc-Si i-layers, and correlate the 'film' properties with features of corresponding solar cells.

Device (nc-Si absorber) non-uniformity will be described. High efficiency solar cells have only been made with 'near-the-edge' nc-Si absorbers (under plasma conditions very close to the demarcation of amorphous to nanocrystalline transition). An optical technique to probe nc-Si defect density developed at Syracuse University is described together with some preliminary data.

### 5.1 Non-uniformity, micro-structural characterization, and device correlation

The uniformities of i-layer microstructure and its correlation with device-performance were selectively investigated by Raman scattering. Strong spatial variations in i-layer microstructure *and* device properties frequently occur over the 12"x15" substrates, depending on i-layer growth conditions and the uniformity of the seeding layer. As an example, **Figure 10** depicts the linear profile of the intensity ratio of Raman shifts, $I_c/I_a$ (the ratio of signal at 520 $cm^{-1}$ to that at 480 $cm^{-1}$), which can be considered a measure of degree of nanocrystallinity of the i-layer, of an arbitrarily chosen plate (from a deposition run with relatively high RF power). The substantial variation of $I_c/I_a$ is unambiguously accompanied by strong variations in device parameters across the plate. This kind of behavior is typical of plates made with non-uniform i-layer thickness distribution. The thickest-film area tends to be mixed-phase in nature ($I_c/I_a < 1$), while other areas are nanocrystalline as indicated by Raman and device characteristics. The highest solar cell efficiency is invariably found where the Si:H i-layer sits on the 'shoulder' of transition from mixed-phase to higher-nanocrystalline state (the so-called 'near-the-edge' type of nc-Si films). Inferior device performance has been observed in areas that contain either mixed-phase Si:H or nc-Si of higher degrees of nanocrystallinity (compared to 'near-the-edge' materials).

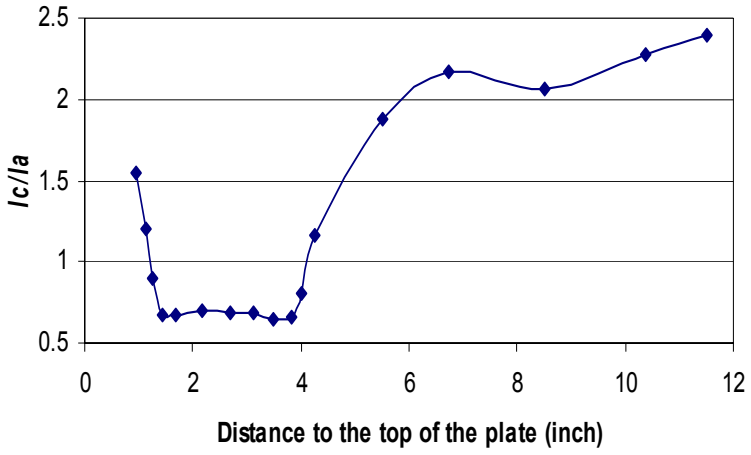


**Figure 10** Raman scattering derived nanocrystallinity versus sample position

The nc-Si solar cells of high degree of nanocrystallinity consistently exhibit low FF and low $V_{oc}$. The red-light response is high only under strong reverse electrical bias, suggesting poor carrier collection (enhanced trapping and recombination). That is, the $J_{sc}$ is actually lower in a nc-Si solar cell with an absorber of higher $I_c/I_a$ ratio in spite of its superior optical absorption compared to the 'edge' type nc-Si i-layer. **Figure 11** presents the variation of $V_{oc}$ with Raman scattering

derived $I_c/I_a$ ratio for a collection of Si:H solar cells from different deposition runs. Among devices prepared by the same seeding technique (which has had overwhelming influence over device properties including $V_{oc}$), lower $V_{oc}$ generally corresponds to higher nanocrystallinity of the absorber (with stronger red-light response under bias). Low FF and low $V_{oc}$ also occur concurrently in solar cells with higher nanocrystallinity in contrast to devices with mixed-phase or 'near-the-edge' nc-Si absorbers (which tend to show high $V_{oc}$ but low FF, or low $V_{oc}$ but okay FF). Our findings are consistent with reports from other groups working on nc-Si solar cells.

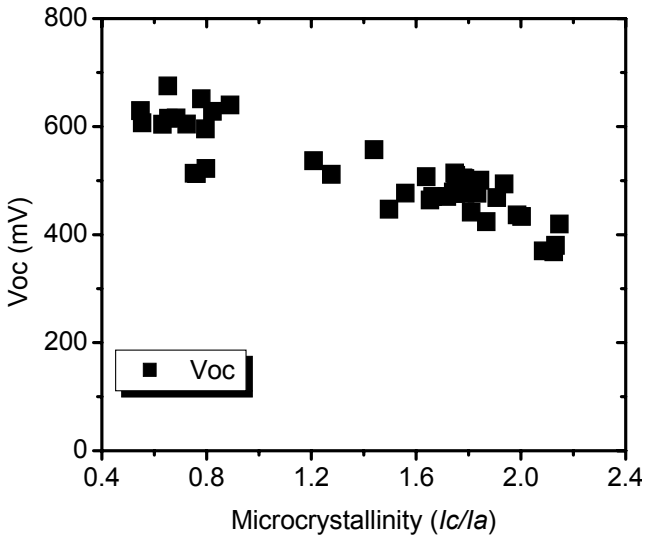


**Figure 11** Variation of $V_{oc}$ with $I_c/I_a$ ratio of the Si:H i-layer

In addition to pronounced thickness variations, we frequently observe variations of surface 'texture' (the apparent haze or 'milkiness') over the deposited plates. Part of the changes in surface appearance may by caused by non-uniformity in seeding (as opposed to that of i-layer deposition), which has been noted under some conditions. Uniform deposition of nc-Si:H *films* certainly appears attainable, but we have yet to find ways to uniformly growing good nc-Si:H *devices*. Device uniformity tends to get worse with increasing growth rate or higher $SiH_4$ depletion. A limitation of our reactor is the supply gas distribution that leads to non-uniform $H_2$ dilution profile (variation in the effective R) across the substrates under high plasma excitations. Since optimal nc-Si:H solar cells are obtained under conditions 'near the edge' or boundary of amorphous to nanocrystalline phase transition (a very narrow processing window indeed for large area deposition), spatial variations in $SiH_x$ concentrations (among other things) naturally lead to vastly dissimilar degrees of i-layer nanocrystallinity over the substrate area.

A number of samples have been characterized by glancing angle x-ray diffraction (XRD) at NJIT. The XRD spectra of three solar cells with nanocrystalline or mixed-phase Si:H i-layers are shown in **Figure 12**. The XRD peaks at 2θ of 28.5° and 47.4° were taken as signatures of Si (111) and Si (220) planes, respectively. For the mixed-phase Si:H sample, no Si peaks were detected even though a weak signal at 520 $cm^{-1}$ was seen in its Raman scattering spectrum. The sample with an $I_c/I_a$ value of 1.88 ('near-the-edge' nc-Si) has the best PV performance among the

three samples, and it shows strong Si (220) preference over Si (111). The sample with higher nanocrystallinity ($I_c/I_a$=2.39), which is thinner than the 'edge' sample, displays a strong XRD signal at Si (111) and a comparatively weak signal at Si (220). The average 'grain sizes' of the two nc-Si:H samples have been roughly estimated to be 90 Å and 130 Å, respectively. Our data are consistent with other reports that the Si (220) planes orientation is favored by good solar cells (presumably with the 'edge' type nc-Si absorbers). It is unclear if poor nc-Si absorber is always accompanied by a dominant Si (111) peak over Si (220) in its XRD spectrum.

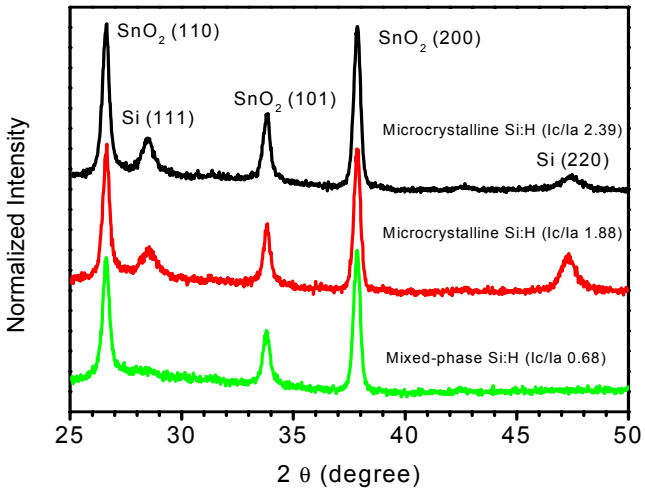


**Figure 12** XRD data of mixed-phase and nc-Si solar cells

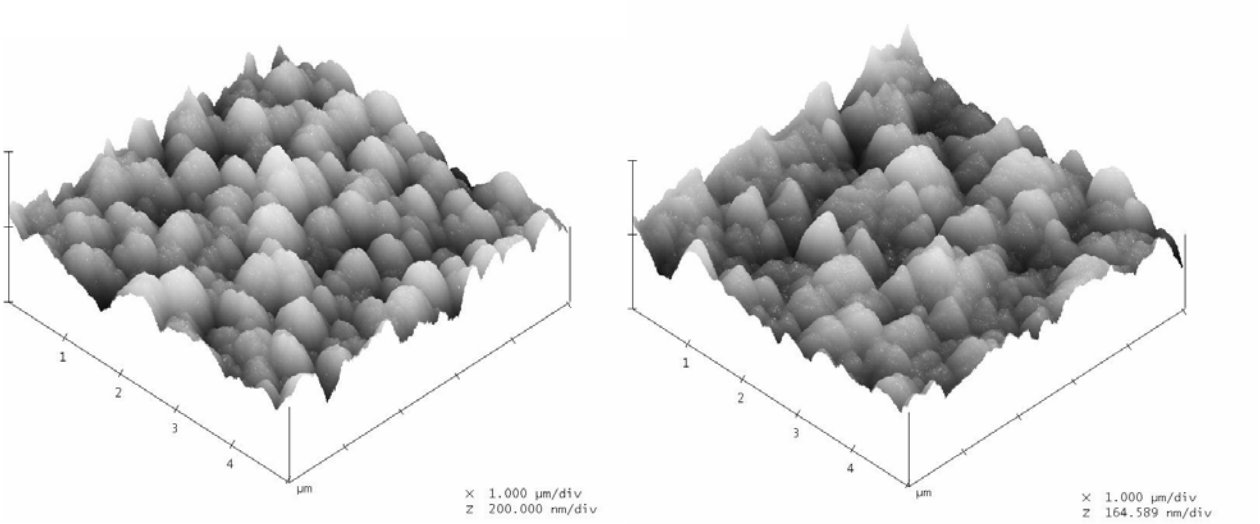


Mixed-phase Si:H nc-Si:H

**Figure 13** AFM images of two solar cells with different i-layer properties

Different surface morphologies have been observed by atomic force spectroscopy (AFM) for selected samples. **Figure 13** depicts the AFM-derived surface profiles of two solar cells with nc-Si:H and mixed-phase Si:H absorbers, respectively. Less-regular surface morphology and lower surface roughness were seen in solar cells with nc-Si:H i-layers compared to that observed in solar cells with mixed-phase Si:H i-layers. An increase of surface roughness (RMS, root mean square) value has been observed in the phase transition regions ('borderlines' between the mixed-phase and the nc-Si regions). Compared to areas with optimal $I_c/I_a$ values ('near-the-edge' films with good solar cell properties) which exhibit the lowest surface roughness, higher-nanocrystalline areas show slightly elevated surface roughness.

In summary of this subsection, strong correlations among device performance, i-layer structural properties, and the related uniformity behavior of Si:H solar cells have been established by direct structural characterization using Raman scattering, XRD, and AFM techniques. Stable, high performance nc-Si:H solar cells contain nc-Si i-layers grown near the nanocrystalline-to-amorphous phase transition (or 'near-the-edge') where an optimal range of nanocrystallinity represented by moderate $I_c/I_a$ values has been observed. Compared to solar cells containing i-layers of higher degrees of nanocrystallinity, the 'near-the-edge' absorbers (most favored by solar cells) having moderate nanocrystallinity exhibit preferential orientation corresponding to Si (220) planes, less-regular surface morphologies, and lower surface roughness.

## 5.2 Why 'near-the-edge' nc-Si makes better solar cell absorber?

Our device and structural data are consistent with the notion that the best (and stable) nc-Si:H solar cells comprise i-layers deposited near the border of nanocrystalline-to-amorphous (mixed-phase) transition. Such 'near-the-edge' nc-Si films have moderate $I_c/I_a$ ratio and smaller 'grain' size than the more crystalline films grown by, e.g., higher $H_2$ dilution. The extreme sensitivity of solar cell performance to the degree of nanocrystallinity of nc-Si i-layer is a major road block for device optimization, and for large area device uniformity (module fabrication). A great deal of variation in nc-Si absorber thickness can be tolerated in large-area module fabrication (since there is no penalty of light-induced instability proportional to absorber thickness), but not the excessive spatial variations in efficiencies typically observed with our present processes. Is higher degree of nanocrystallinity *fundamentally* incompatible with good device performance?

It is essential that some basic understanding (or conjecture) be established as to why higher nanocrystallinity results in inferior solar cells versus that of 'near-the-edge' nc-Si:H. We are of the opinion that, for nc-Si solar cell technology to be commercially viable (reproducible, uniform, high-throughput processes using relatively simple, low-cost manufacturing equipment), the PECVD processing window for nc-Si absorber needs to be drastically enlarged from its present, stringent requirement of producing '*near-the-edge*' material. What is wrong with nc-Si materials of higher degree of nanocrystallinity than that of 'near-the-edge' variety? Is it more efficient contamination in the 'grains' (as opposed to the 'grain boundaries')? Insufficient hydrogen passivation of defects along 'grain boundaries' (loss of H coverage)? Unidentified deterioration of carrier transport in the film growth direction? Poor interface compatibility or higher density of p/i interface defects? Or something else? A more transport-friendly columnar structure has been speculated to exist in 'near-the-edge' type nc-Si. Perhaps, 'near-the-edge' nc-Si is required only near the p/i interface, and not across the entire absorber thickness. We just do not know.

Some ideas can be tried to broaden the processing window for nc-Si films, including ways of independent control of atomic hydrogen for the *dual* roles of defect passivation and promotion of

crystallite growth; the use of different gas/feedstock mixtures and/or diluents (e.g., adding some inert gas); variations in 'etching' chemistry (e.g., using halogens from $SiF_4$ or $SiCl_2H_2$) that does not rely solely on hydrogen; modulation of plasma conditions (e.g., gas flow and/or power level grading); lower substrate temperatures; very high TCO texture; and alloying of nc-Si. These tricks may help to prevent the nc-Si material from becoming 'too nanocrystalline'.

## 5.3 Optical absorption of nc-Si i-layers by infrared photocurrent spectroscopy

In addition to developing advanced deposition system and process technology, we also proposed in Phase I of the project to develop characterization techniques for the study of intrinsic nc-Si:H films and solar cells, which can be used as a guidance for optimizing the fabrication process of nc-Si materials and solar cells. This subsection describes the successful efforts in establishing such a technique by A. Rafik Middya, Eric A. Schiff, and Jianjun Liang at Syracuse University.

In spite of the tremendous progress in nc-Si:H solar cell technology over the last ten years, the electronic transport in devices and the critical factors controlling the performance of solar cells have not been properly understood. Conventionally, the constant photocurrent method (CPM) and solid state photocarrier grating (SSPG) technique have been used to estimate the defect density and minority carrier transport in intrinsic nc-Si layers respectively. However, both of these techniques provide information only about standalone films, but not actual devices. The carrier transport direction is different in the films (coplanar) than that of real-life solar cells (perpendicular to the substrate). Hence, we propose infrared photocurrent spectroscopy (IPS) as a more appropriate method to estimate defect density in intrinsic nc-Si:H layer *directly* in solar cell configuration.

In the IPS technique, an intensity-modulated (chopping frequency = 1 kHz) light beam from a monochromator is incident on the sample from the glass substrate side. Any light not absorbed by the various Si:H layers (p, seed, i, n) is partially reflected from the back Al contact. The modulated photocurrent, $J_{sc}(h\nu)$, of the solar cell is detected by a lock-in amplifier. The $J_{sc}(h\nu)$ spectrum is acquired by a computer. A thermopile was used to calibrate the photon flux $F(h\nu)$. Two optical filters have been used to measure optical absorption over the wide range of photon energy (3.2 eV to 0.8 eV). One filter is used to cut off all the light below 780 nm, and another filter is used to block all the light below the wavelength 1000 nm. Assuming that $J_{sc}$ is equal to the area density of photogeneration within the intrinsic layer of the solar cell, we can convert the photocurrent signal to optical absorption coefficient using the expression $J_{sc}(h\nu)/(\chi eF(h\nu)d)$, where $e$ is the electronic charge, $F(h\nu)$ is the photon flux, $d$ is the thickness of the intrinsic layer, and $\chi$ is a multiplication factor to take into account the reflection from the Al back contact. For simplicity, here we assume $\chi$ to be a constant, and we use a value $\chi = 1.4$ for later discussions.

We have measured by photocurrent spectroscopy three sets of nc-Si:H solar cells prepared at EPV using three different seeding methods. The samples have the standard device structure as described earlier: soda-lime glass/$SnO_2$/p/i/n/Al. The thicknesses of the nc-Si i-layers are in the range of 1.2-1.5 μm. Selected solar cell parameters for the samples are given in **Table 5**.

The IPS derived optical absorption spectra of the absorber layers of four solar cells (two samples from each run of R130-1 and R140-3), are shown in **Figure 14**. The labels '130-1-e' and '130-1-f' refer to two adjacent, different 'dots' made on the same plate R130-1. Samples from R141-1 had peeled off during measurements. In the same plot, the optical absorption spectra of standard amorphous silicon (a-Si:H) and crystalline silicon (c-Si) are also shown for comparison.

| Run I.D. | Nucleation method for i-layer | $V_{oc}$ | $J_{sc}$ | FF | Effi. |
|---|---|---|---|---|---|
| | | (V) | ($mA/cm^2$) | (%) | (%) |
| R130-1 | p-seeding on a-SiC p-layer | 0.50 | 13.6 | 55 | 3.7 |
| R141-1 | i-seeding using high $H_2$ dilution to $SiH_4$ | 0.52 | 14.7 | 47 | 3.6 |
| R140-3 | p-seeding with thicker 'nc-Si' p-layer | 0.48 | 13.2 | 65 | 4.1 |

**Table 5** Properties of nc-Si solar cells studied by infrared photocurrent spectroscopy

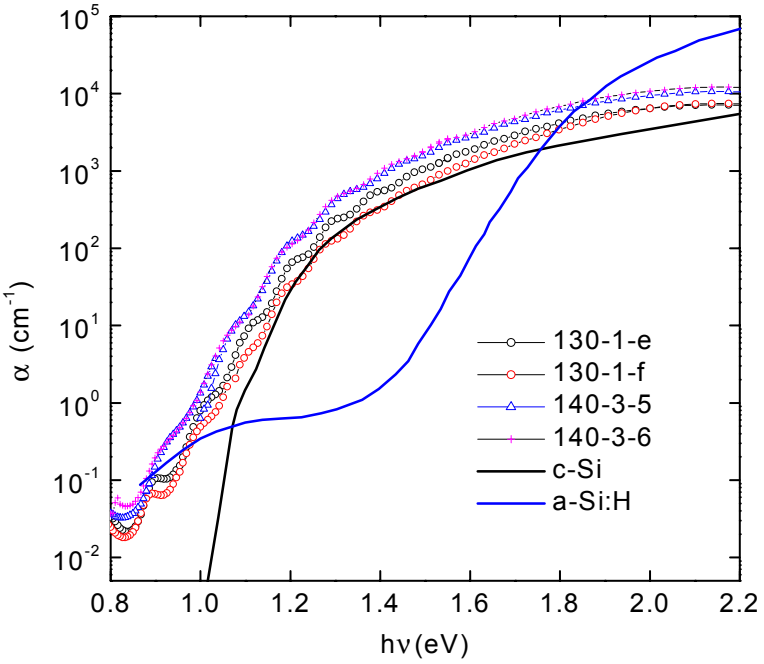


**Figure 14** Optical absorption spectra of intrinsic layers of selected nc-Si:H solar cells

It can be seen from figure 14 that the spectral dependence of α of the nc-Si:H i-layers of all four solar cells resemble that of c-Si, and they are quite different from that of a-Si:H. In other words, we can state that, in these nc-Si:H solar cells, the photogeneration mainly occurs in the crystalline grains. The shape of the nc-Si absorption curves differs from that of c-Si for photon energies below 1.1 eV. The low-energy absorption of these samples appears to flatten near 0.8 eV, with a 'saturation' value of α at 0.8 eV around $5x10^{-2}$ $cm^{-1}$, which is in the same range as that of best nc-Si:H films reported in the literature (measured in co-planner configuration). It has been demonstrated that α at 0.8 eV reflects Si dangling-bond related defects in nc-Si films [9]. Therefore the defect densities of EPV's nc-Si samples, measured in solar cell configuration, are similar to that of best nc-Si:H films measured by CPM. However, optical absorption estimated

in co-planner configuration always exhibits higher values than sandwich (CPM) configuration [10]. Thus, EPV's nc-Si devices may have slightly higher defect density than that of the best nc-Si films reported in the literature, *if* one does not correct for optical enhancement effect (which is stronger at longer wavelengths, not a constant) due to texturing and Al back contact in solar cells.

Slightly higher defect density (compared to the best reported in the literature) of EPV's sample R130-1 cannot account for the low FF of ~ 0.55. During the fabrication of solar cells, H-plasma seeding treatments on p-type a-SiC:H were performed before the growths of i-layers. Such seeding related process may induce lower extended defects ('twins and dislocations') within columnar grains than in i-layers without proper seeding procedure. The IPS data suggest that EPV's samples have low density of silicon dangling bonds (which are presumably concentrated at the 'grain boundaries', if the 'grain' and 'grain boundary' concepts are valid at all in nc-Si material). From earlier sections, the inferior performance of most of the nc-Si:H solar cells is attributable to inadequate seeding procedure (interface defects), rather than some 'bulk' defects.

A noteworthy feature of figure 14 is the variation of optical absorption ($\alpha$), at a given photon energy ($h\nu$), among the nc-Si:H samples for $h\nu \approx 1.2 - 2.6$ eV. Moreover, interference fringes have been observed for all samples at $h\nu < 1.5$ eV. This type of variation in $\alpha$ (for the same $h\nu$) has not been widely reported, or at least the observed differences in the literature have not been so prominent for PECVD nc-Si:H films having varying crystalline fraction ($X_c$). However, there have been reports describing variation of $\alpha$ of HWCVD samples having different microstructures (i.e., different $X_c$) [11]. It is generally observed that the surface of nc-Si films prepared by hot-wire CVD is more textured than PECVD films, i.e. internal texturing (suitable for light trapping) of the two types of films can be quite different. Generally, $\alpha$ in the visible as well as in the infrared region may vary if i) crystalline fraction ($X_c$) varies or ii) internal texturing of the films varies with different H-dilution (or silane concentration). Thus, the large variations of $\alpha$ in the infrared region of EPV samples can be caused by i) variation in $X_c$ (for samples from different runs, or of different film thickness), or ii) different internal texturing of the films which might be induced by small variations in the seeding surface prior to nc-Si i-layer deposition.

## 6.0 Other Topics: Tunnel Junction for Tandem Cells, and Back Contact

This section deals with some device topics not directly related to nc-Si PECVD processes.

### 6.1 Tunnel junction for tandem solar cells

To be properly prepared to fabricate a-Si:H/nc-Si:H double-junction solar cells, we began to develop tunnel junction processes using the simpler a-Si:H/a-Si:H device configuration in the 3rd quarter of Phase I, as it is easier to evaluate the tunnel junction using a-Si:H rather than nc-Si as the bottom cell in a dual-junction device. Most of the tunnel junction experiments were devoted to fabricating nc-Si n-layers (n1 layer for the top junction), using seeding and growths methods similar to those used for nc-Si i-layers described earlier. The seeding and growth of nc-Si n-layers involved relatively high concentration of $PH_3$ in the gas mixtures. These devices had worked well, with FF of 74-75% in some a-Si/a-Si tandem solar cells of well balanced currents from top and bottom junctions. However, we soon realized that a tunnel junction process suitable for a-Si:H/a-Si:H tandem devices may not necessarily be acceptable for a-Si:H/nc-Si:H 'micromorph' type devices of superstrate configuration due to phosphorus cross-contamination

described earlier (Sec.4.2), as nc-Si i-layer is much more sensitive to residual contaminants than a-Si:H i-layer. Prolonged use of $PH_3$, especially under high RF power plasma, caused more evident contamination in subsequent nc-Si runs even after extended periods of bake-out and high-vacuuming. It is worth noting that in a number of tandem solar cells with presumably nanocrystalline Si n-layers as tunnel junctions, $V_{oc}$ values were substantially lower than the 1.6 V obtained for reference a-Si/a-Si solar cells on low-cost $SnO_2$ substrate. It appears that some highly nanocrystalline Si n-layers are not suitable for tunnel junction application.

To minimize contamination of the bottom nc-Si i-layer, we have been investigating tunnel junction recipes that entail less $PH_3$ exposure to the system compared to that needed for nc-Si n-layer. Such techniques as relatively-heavily doped $n^+/p^+$ junctions have been explored, so has the use of a $n^+$ layer by itself (with short $n^+$ deposition time). The amorphous Si based tunnel junctions have worked OK but not great, as the FF of the a-Si/a-Si tandem test devices were in the mid to high 60% range. We also observed that the presence of a thin, slightly n-type nc-Si layer (as an unintentional tunnel junction) sandwiched between n1 and p2 layers greatly reduced the $V_{oc}$ and FF of the tandem solar cells.

As a test for amorphous Si based tunnel junction, we made an a-Si/nc-Si tandem solar cell trial deposition (run #R253) using p-seeding method for the bottom nc-Si junction. The following solar cell parameters were obtained for this run: $V_{oc}$=1.20 V, $J_{sc}$=7.4 mA/cm$^2$, FF=63.2%, efficiency=5.6% (using Al back contact and standard, commercial AFG $SnO_2$ superstrate). The QE spectrum indicated significant optical loss in the tunnel junction with low peak QE value. The FF and $V_{oc}$ were both quite low. Our search for a good tunnel junction compatible with low-contamination requirement is continuing.

For single junction nc-Si solar cells, the use of a nanocrystalline Si n-layer (grown directly on the nc-Si i-layer), instead of the standard amorphous Si (a-Si) n-layer, did not lead to appreciably different device behavior. Also, preliminary tests show that the use of a wider bandgap n-layer (a-SiC:H) has no marked impact on the nc-Si devices. We did observe that when the n-layer thickness was greatly reduced (< 150-200 Å), solar cell performance fell dramatically.

## 6.2 Back contacts and issues of optical engineering

As stressed earlier, low $J_{sc}$ has been the most notable weakness of our nc-Si (and a-Si) devices. A main reason for the low $J_{sc}$ is the use of weakly-reflecting Al back contact. The other obvious reasons include high optical absorptions by the commercial $SnO_2$ and by the 3-mm thick soda-lime glass substrate, low-texturing of the front contact, i-layers that are neither highly nanocrystalline nor very thick, and the aforementioned poor transparency of the p-seed layers. We have compared the QE spectra of co-deposited nc-Si solar cells with Al and ZnO/Al back contacts made by magnetron sputtering. **Figure 15** compares QE spectra of three nc-Si solar cells made with the same recipe. Two of the samples have the same commercial LOF TEC7 $SnO_2$ front contact but different back contact of either Al or ZnO/Al. The third sample has the special, research grade Asahi type 'U' $SnO_2$ front TCO, and ZnO/Al back contact. An increase in $J_{sc}$ of ~ 2 mA/cm$^2$ has been seen with ZnO/Al back contact versus Al alone, mainly due to a boost in the long-wavelength response. As a reference, the increase in $J_{sc}$ is about 7-8% for a-Si:H single junction solar cells when ZnO/Al is used instead of Al alone, versus a gain of > 12% for nc-Si single junction cells. The higher texture and better transmission of the Asahi $SnO_2$ (on a more transparent, thinner glass substrate) account for the higher red-light response in the third nc-Si solar cell in figure 15. The FF of the cell with Asahi $SnO_2$ front contact is actually quite

low (~60%) due to lack of optimization of the p-seeding recipe on the more textured substrate (compared to the low-haze LOF $SnO_2$). Up to now, our default (routine) back contact is Al for its ease of deposition and good uniformity.

To reap the benefit of ZnO/Al back contact, we have started to fine-tune the ZnO sputtering process for more repeatable, low-resistance contact to a-Si:H n-layers. To this end, a shutter has been installed in our R&D sputtering machine such that proper target conditioning (pre-sputtering after the system's exposure to air upon sample loading and unloading) can be performed prior to ZnO deposition on to the solar cells. We expect to make more routine ZnO/Al back contacts on nc-Si single junction and a-Si/nc-Si tandem solar cells once a reliable process has been instituted. Further down the road, we intend to evaluate silver (Ag) as part of the back reflector (in place of, or in addition to, Al). Also planned, for the longer term, is the development of LPCVD ZnO as the front contact, as ZnO is a popular choice among the many groups working on nc-Si PV technology.

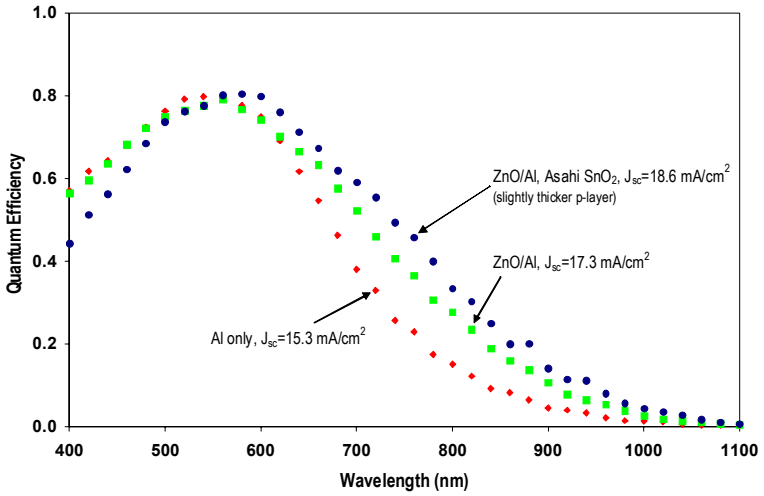


**Figure 15** QE spectra of three solar cells with Al or ZnO/Al back contact

We have made a few attempts, using a-Si:H absorber, to create texture or high-haze in the solar cells without success. Traditionally, the degree of texture in thin film solar cells (needed for more efficient light trapping) relies almost entirely on the roughness of the substrate (in our case, the superstrate TCO or $SnO_2$). We have found that, in many of our nc-Si depositions, the mixed-phase areas exhibit very 'milky' appearance due to Si:H deposition-enhanced surface roughness, evidently with superior light trapping effect (especially at the boundaries between the mixed-phase region and the nc-Si area). The 'hazy' area has a darker color when viewed against visible light (more absorption). This effect is more pronounced on low-textured $SnO_2$ (e.g., LOF TEC7), and is mostly absent in higher-haze $SnO_2$ (e.g., newer type AFG $SnO_2$). We believe that PECVD-enhanced texturing of the absorber layer is an important topic for future research, as it promises to substantially reduce the reliance on the front TCO for enhanced capture of light.

## 7.0 Summary and Future Plan

In summary, the search for good seeding techniques and the struggle with device reproducibility (process control) accounted for most of the activities at EPV in Phase I. The p-seeding approach has proved to be superior to i-seeding for preparing single junction nc-Si solar cells. Phosphorus contamination has been a very difficult issue for our single-reactor/single chamber operation that puts severe limitations on operating procedures and plasma parameters. At Syracuse University, the setup for the combined plasma and hot-wire CVD has been completed, and the infrared photocurrent spectroscopy technique has been developed as a useful device characterization tool.

Relatively efficient p-i-n nc-Si:H single junction solar cells with excellent stability have been prepared in a low cost, single chamber, non-load-locked RF-PECVD system on inexpensive $SnO_2$ substrates using Al back contact. The seeding procedure has had the biggest impact on the devices. Dopant cross contamination has often posed a great challenge. Correlations between device performance and the i-layer microstructure indicate a very narrow processing window for *optimal* nc-Si:H absorber, which is grown near the 'edge' of amorphous to nanocrystalline phase transition. The 'near-the-edge' material requirement severely hinders improvements in nc-Si:H PV devices and their uniformity.

While we are enormously encouraged by some of the solar cell data which have demonstrated the viability our *unconventional*, low-cost approach to fabrication of nc-Si solar cells, we are mindful of the tremendous difficulties that still lie ahead. In particular, we must further validate our approach by optimizing the seeding techniques, improving the uniformity of nc-Si devices, gaining better reproducibility by suppressing cross-contamination, developing a tunnel junction compatible with the synthesis of a-Si/nc-Si tandem solar cells, and ultimately, demonstrating high conversion efficiencies from a-Si/nc-Si tandem solar cells and PV sub-modules produced using manufacturing procedures as we proposed to NREL for the present subcontract. We have only taken the first step in a long and arduous journey. We now reiterate the high-priority areas and key questions for future activities:

- Find a robust p-seeding technique (on $SnO_2$ TCO) that has low optical loss.
- Is p-seeding fundamentally superior to i-seeding (in the context of single-reactor system)?
- Improve nc-Si device uniformity (not necessarily *thickness* uniformity) over large areas. Both seeding and nc-Si i-layer growth determine the properties of the resulting solar cells.
- Why nc-Si of higher degree of crystallization is *inferior* to 'near-the-edge' nc-Si for solar cell performance despite its larger 'grain size' and higher $X_c$ (stronger optical absorption)? This central question has a direct bearing on device-performance and uniformity issues.
- Effective tunnel junction that satisfies the stringent demand for contamination control for tandem cells (far more difficult than single junction devices in single-chamber operation).
- More sophisticated optical engineering for higher $J_{sc}$: ZnO/Al or ZnO/Ag back contacts; Higher textured front contact; More transparent TCO/glass; ZnO front contact.
- Higher deposition rates compatible with good, uniform device performance.
- Study nc-Si materials prepared by the combined plasma and hot-wire CVD method.
- Evaluate nc-Si absorber properties, in device configuration, using instructive techniques such as infrared photocurrent spectroscopy. Develop additional device diagnostic tools.

## References


[1] A. Shah, J. Meier, E. Vallat-Sauvain, C. Droz, U. Kroll, N. Wyrsch, J. Guillet, and U. Graf, *Thin Solid Films* Vol. 403-404, p.179-187 (2002).

[2] J. Meier, H. Keppner, S. Dubail, Y. Ziegler, L. Feitknecht, P. Torres, Ch. Hof, U. Kroll, D. Fischer, J. Cuperus, J. A. Anna Selvan, & A. Shah, *Proc. WCPEC-2*, Vienna, Vol.I, p.375 (1998).

[3] K. Yamamoto, M. Yoshimi, Y. Tawada, Y. Okamoto, and A. Nakajima, *Tech. Digest 11th Internat. PV Sci. & Engineer. Conf.*, Sapporo, Japan, p.225 (1999).

[4] T. Roschek, T. Repmann, J. Mueller, B. Rech and H. Wagner, *Conf. Rec. 28$^{th}$ IEEE PVSC*, p.150 (2000).

[5] J. A. Anna Selvan, "ZnO for Thin Film Solar Cells", published by UFO Atelier fur Gestaltung & Verlag, Germany, ISBN 3-930803-60-7 (October, 1998).

[6] A.E. Delahoy, Y.-M. Li, J.A. Anna Selvan, L. Chen, T. Varvar, and H. Volltrauer, *Conf. Proc. "PV in Europe"* (October 7-11, 2002, Rome, Italy), p.444.

[7] A. R. Middya, A. Lloret, J. Perrin, J. Huc, J. L. Moncel, J. Y. Parey and G. Rose Mater. Res. Soc. Proc. 377 (1995) 119.

[8] J. E. Bouree, J. Guillet, C. Grattepain and J. Chaumont, Proc. in the 2$^{nd}$ International Conference on Cat-CVD (Hot-Wire CVD) Process, 2002 (in Press).

[9] M. Vanecek, A. Poruba, Z. Remes, J. Rosa, S. Kamba, V. Vorlicek, J. Meier, A. Shah J. Non-Cryst. Solids 266-269 (2000) 519-523.

[10] T. Unold, R. Brueggemann, J. P. Kleider, and C. Longeaud, J. Non-Cryst. Solids 266-269 (2000) 325.

[11] S. Klein, F. Finger, R. Carius, H. Wagner and M. Stutzmann, Thin Solid Films (2001) 305-309.